SKB TECHNICAL REPORT 92-35

Calibration and validation of a stochastic continuum model using the Finnsjön dipole tracer test. A contribution to INTRAVAL phase 2.

Kung Chen Shan[1], Vladimir Cvetkovic[1], Anders Winberg[2]

[1] Royal Institute of Technology, Stockholm
[2] Conterra AB, Göteborg

December 1992

SVENSK KÄRNBRÄNSLEHANTERING AB
SWEDISH NUCLEAR FUEL AND WASTE MANAGEMENT CO

BOX 5864 S-102 48 STOCKHOLM

TEL 08-665 28 00 TELEX 13108 SKB S
TELEFAX 08-661 57 19

CALIBRATION AND VALIDATION OF A STOCHASTIC CONTINUUM MODEL USING THE FINNSJÖN DIPOLE TRACER TEST. A CONTRIBUTION TO INTRAVAL PHASE 2

Kung Chen Shan[1], Vladimir Cvetkovic[1], Anders Winberg[2]

1 Royal Institute of Technology, Stockholm
2 Conterra AB, Göteborg

December 1992

Information on SKB technical reports from 1977-1978 (TR 121), 1979 (TR 79-28), 1980 (TR 80-26), 1981 (TR 81-17), 1982 (TR 82-28), 1983 (TR 83-77), 1984 (TR 85-01), 1985 (TR 85-20), 1986 (TR 86-31), 1987 (TR 87-33), 1988 (TR 88-32), 1989 (TR 89-40), 1990 (TR 90-46) and 1991 (TR 91-64) is available through SKB.

Calibration and Validation of a Stochastic Continuum Model using the Finnsjön Dipole Tracer Test

-

A Contribution to INTRAVAL Phase 2

by

Kung Chen Shan[1)], Vladimir Cvetkovic[1)]
and
Anders Winberg[2)]

[1)] Royal Institute of Technology, Stockholm

[2)] Conterra AB, Göteborg

December 1992

Keywords:

calibration, conditioning, dipole tracer experiment, far-field, Finnsjön, INTRAVAL, parametric, stochastic continuum, transport, uncertainty, validation strategy

Abstract (English)

A realistic semi-synthetic transmissivity field and dipole tracer test conditions similar the actual field test conditions at Finnsjön were used to demonstrate a calibration and validation procedure applied to a stochastic continuum model. A validation strategy was set up to address whether a model calibrated and possibly validated on a local model scale, also is validated when extrapolated to a far-field scale. A generated 2D realization of the material property distribution on a far-field scale, honouring the measured single hole data and also recapturing the characteristics of the field dipole tracer test, was selected as an exhaustive reference field. The results of the simulated dipole tracer test on a local scale and of a far-field natural gradient tracer test were considered as reference field results. A large number (N=100) of conditioned parametric realizations of the studied domain were generated and the dipole tracer experiment was simulated for each realization. The porosity of the 2D aquifer model was used to calibrate the stochastic simulations on a local scale. An alternative calibration using a defined index of deviation was also applied. Subsequently, also the natural gradient tracer test was simulated on a far-field scale for the ensemble of realizations. It was found that the realizations which based on the defined index of deviation compared best with the local scale reference results did not recapture the characteristics of the reference far-field results. It was thus concluded that calibration/validation of a model on a local scale is insufficient for validating the model also on another larger transport scale. In order to reduce the uncertainty in the far-field simulations more data on the corresponding transport scale are required.

Abstract (Swedish)

En realistisk semisyntetisk transmissivitetsfördelning och testförhållanden motsvarande dipolspårförsöket i Finnsjön utnyttjades för att demonstrera en arbetsgång för kalibrering och validering av en stokastisk kontinuummodell. Den uppsatta valideringsstrategin behandlade möjligheten att en modell som kalibrerats och möjligen validerats i lokal modellskala, också kan valideras när modellen extrapoleras till en större (fjärrzons-) skala. En tvådimensionell realisering av materialegenskapsfördelningen i fjärrzonsskala, som inkluderar mätta data från enhålstester och också väl reproducerar karaktäristiska resultat från det utförda dipolspårförsöket i fält valdes ut för att gälla som referensdataset. Resultat från simulerade dipolspårförsök i lokal skala och spårförsök i fjärrzonsskala under naturliga gradientförhållanden, baserade på den utvalda realiseringen av transmissivitet betraktades som referensresultat mot vilka fortsatta simuleringar skall jämföras. Ett stort antal (N=100) av simulerade betingade parametriska realiseringar av den studerade domänen genererades och dipolspårförsöket simulerades för varje realisering. Porositeten som ansatts för den tvådimensionella akvifärmodellen utnyttjades för kalibrering av de stokastiska simuleringarna i lokal modellskala. Ett definierat index för avvikelse från referensresultatet utnyttjades också för en alternativ form av kalibrering. Därefter simulerades också spårförsöket i fjärrzonsskala under rådande naturliga gradientförhållanden i den upprättade ensemblen av realiseringar. Det befanns att de realiseringar som baserat på definierat index uppvisade bäst överensstämmelse med referensresultaten i lokal skala, inte återgav referensresultatet erhållet i fjärrzonsskala. Erhållna resultat visade därför att kalibrering/validering av en modell på lokal modellskala inte är tillräckligt för att också validera modellen på en annan, större transportskala. För att minska osäkerheten i simuleringarna i fjärrzonsskala krävs mera data på motsvarande transportskala.

Contents :

1. Introduction

The treatise of issues pertaining to validation of geosphere groundwater flow and radionuclide transport models constitutes the major objective of the international INTRAVAL study. The purpose of the study is to increase the understanding of how mathematical models can describe various geophysical, geohydrological and geochemical phenomena of importance for radionuclide transport from a repository for radioactive waste to the biosphere. In doing so, information from laboratory and field experiments as well as from natural analogue studies have been used as input to mathematical models in an attempt to validate the underlying conceptual models and to study model validation. The ambition of INTRAVAL has been to address both validation of models with regard to acting processes, and of site-specific systems.

Ten test cases are included in the Phase 2 of INTRAVAL, making up four working groups. Working group no. 2 lead by C.F. Tsang (LBL) analyses three test cases which address heterogeneous fractured rock (crystalline and sedimentary);

- Finnsjön
  * converging tracer test
  * dipole tracer test
- Stripa
  * three-dimensional migration experiment
  * site characterization and validation experiment
  * channelling experiment
- Wipp-2
  * flow and transport experiments

The conceptual approaches employed to test the cases analysed by working group 2 have until recently exclusively been limited to analytical models based on the advection-dispersion model (Goblet 1992, Kimura and Manukate 1992, Hautojärvi et al 1992, Moreno and Neretnieks 1992 and Grindrod and Worth 1992), numerical models em-ploying the deterministic continuum (Andersson et al 1992) and stochastic description using the discrete fracture network approach (Yamashita and Kobayashi 1992). However, recently the stochastic continuum approach (Cliffe et al, in prep) and also fractal analysis have been employed to the WIPP-2 test case (Grindrod and Capon 1991).

2. Validation aspects

The work presented in this report constitutes a contribution to the validation of models describing groundwater flow and solute transport in heterogeneous media as applied to the tracer experiments performed at Finnsjön. Since analytical, deterministic continuum and fracture network models have been applied to these test cases, the incorporation of the stochastic continuum could provide additional building blocks to the validation process of the test case(-s).

Several comprehensive review papers on the validation issue within the groundwater flow/radio-nuclide transport have recently been presented (Tsang 1991 and Neuman 1992). Both Tsang (1991) and Neuman (1992) differentiate between validation in a *generic* sense as opposed to validation in a *site-specific* sense. The generic aspect of model validation focuses on the specific process which is modelled. Tsang argues that the (single) process studied should be identified, conceptualized and coded. The model (conceptualization and code) is then applied to an experiment where the process is active. The calculated results are compared with measurements. If the agreement is satisfactory, the model is said to be validated with respect to the specific process. Neuman (1992) in addition requires that 1) the scale of application of the process should be stated, or 2) that this scale's relationship to technically feasible measurement scales is given, and 3) how the process scale relates to the scale of numerical discretization, and 4) the quality and quantity of data on relevant supports are stated. Neuman (1992) concludes that "by generic validation of geosphere models one must understand the experimental verification of phenomenological relationships postulated between parameters and state variables on well-defined supports in a particular rock type".

With a site-specific system, Tsang (1991) implies a multiple process system including structure (geometry) and boundary/initial conditions. Once the processes are identified they can be used to simulate the system with subsequent comparison between simulated and measured response. If the correspondence is good the model(-s) are "said to be validated with respect to this particular site, within a range of applications determined by the range of field observations studied". Neuman (1992) further state that "validation of local phenomenological relationships is necessary but insufficient to render models of subsurface flow and transport believable". In addition, one "must validate not only the description of local phenomenology but also the manner in which this description is extended by the model into untested portions of the geologic complex and onto larger scales". This latter statement eludes to the "validity" of extrapolating a model validated on eg. a local scale to far-field conditions.

With regard to theoretical models that predict state variables under data uncertainty, based on stochastic concepts which consider the geostatistical structure and support size of constitutive parameters, they must also be validated generically (Neuman 1992). In addition Neuman (1992) argues since this type of models deal explicitly with data uncertainty, "their validation requires experiments on scales much larger than the local support size, and the collection of local data at sufficiently numerous points in space-time to constitute a statistically meaningful sample".

Tsang (1991) eludes to other possible means of validation with regard to stochastic models presented by Sargent (1984). The first one being *internal validity* which relates to the stochastic variability in the model output. A high degree of variability may cause the model's results to be questionable and may require a redefinition of the appropriate quantity of interest, ie. the appropriate performance measure. The second being *Turing tests* which may be regarded as a part of a peer review. People with site-specific knowledge are asked whether they can discriminate between model output and field observations.

In addition to the review papers discussed above, two applied papers bringing in new approaches have been presented by Luis and MacLaughlin (1992) and Ababou et al (1992).

Luis and McLaughlin (1992) introduce a more formal stochastic approach to validation through hypothesis testing of model error following ample stochastic description of 1) measurement error and 2) spatial heterogeneity. The authors conclude that their approach can identify model deficiencies and provide standards for model performance.

Ababou et al (1992) discuss basic model performance measures but in addition, recognizing the diversity in spatially distributed modelling approaches, also propose measures of *model complexity* and of the *amount of information* inherent in the model predictions. One of these measures is the *spatial degree of freedoms* which is a function of material- and boundary heterogeneities in the model. Another being the *quantity of information* or entropy, which depends also on precision. The authors conclude that <u>full</u> validation is not possible in practice, it is more appropriate to define a <u>degree</u> of validation. This relates to Neuman's (1992) observation that it is more appropriate to refer to the <u>better</u> model among a set of models, rather than specifying the <u>best</u> or ultimate model.

Our choice is the stochastic continuum approach, which with regard to the numerical models employed can be said to constitute a midway compromise between the ordinary deterministic continuum and the discrete fracture network analysis. The validation strategy taken (after Davis and Goodrich 1990) is as follows;

1) Definition of validation issue.

2) Selection of experiments and experiment scales (Finnsjön dipole experiment and planned, yet not performed natural gradient tracer test)

3) Selection of a geometrical conceptual model (2D confined aquifer)

4) Definition of a realistic exhaustive reference transmissivity field on the basis of the geostatistics of available data, comparison of reference data set geostatistics with that of the input data.

5) Local scale (dipole test) and far-field (natural gradient test) flow and transport analysis of reference transmissivity field.

6) Generation of 100 realizations of the studied domain.

7) Simulation of dipole tracer test in each generated transmissivity field.

8) Calibration on the basis of porosity and aquifer thickness.

9) Alternate calibration in terms of selecting the realization(-s) that provides the best fit between simulated breakthrough and the breakthrough of the reference field (using defined index of deviation).

10) Simulation of a natural gradient tracer test in the 100 realizations already produced under point 4).

11) Analysis of effect of adding more conditioning points on local- and far-field scale simulations.

12) Comparison between reference natural gradient breakthrough and simulated results. Is calibration on a local (test) scale sufficient for a model to be also validated on a larger (test) scale? Discussion.

By employing the stochastic continuum approach we acknowledge the heterogeneous nature of the fractured crystalline rock. The validation issue is consequently **whether the stochastic continuum approach can successfully be used to validate transport of tracer in fractured crystalline bedrock, and** eluding to a recent discussion by Neuman (1992) we explore **specifically whether a stochastic continuum model calibrated on a local scale can be validated on a larger scale.** In other words, is calibration/validation on a local (test) scale sufficient for a model also to be validated on a larger (test) scale?

3. Reference field

It has been recognized that when exploring the stochastic approach it is desirable to have one or more benchmark or "reference" results which can be used to verify the effectiveness of a particular method or approach. In most cases, a set up model needs calibration to find the most suitable parameters. In terms of groundwater flow and solute transport, usually the head distribution and breakthrough curves measured in the field, respectively, are used as "reference" results for calibration.

In the case of Finnsjön tracer tests, only one scale of testing has been utilized, hence, if one used the measured test results for calibration, one do not have another set of field measured results on another scale for validation. In most applications the extrapolation of local scale calibrated, and possibly validated, models to a larger scale is a primary goal. The validity and correctness of such an extrapolation is however not straightforward. In view of the lack of a second measurement scale, superior to the one used in the tracer tests, we have instead of using actually measured results for calibration and validation, used a realistic genetic case in order to test our ideas on calibration and validation of a stochastic continuum model. To be as close as possible to the real situation, we have used all the measured data on hydraulic conductivity from the upper high-conductive part of Zone 2 to construct the synthetic reference field. In this synthetic reference field we have performed dipole tracer tests similar to the Finnsjön test and also performed a far-field (natural gradient) test for calibration and validation.

The actual Finnsjön dipole test was performed in a single high-conductive subzone along the upper bound of the 100 m thick subhorizontal fracture zone 2. Eight boreholes penetrating the zone have been hydraulically tested, cf. Figure 1. The mean and variance of $^{10}\log(T)$ values of the measured data are -3.2811 and 0.1543, respectively (based on transmissivities of 6m sections calculated from three 2m injection tests in each borehole centred on the high-conductive subzone), cf. Table 1. The data are assumed to have a lognormal distribution and an isotropic exponential type covariance structure with a 100 m correlation length. Using these statistical parameters, several realizations have been generated and conditioned on the data from the 8 boreholes. The model domain was made 1200 m x 1200 m large so that possible boundary effects are minimized. The domain was discretized into 60x60 blocks with block size of 20 m in order to reduce the computational effort. A constant porosity n=0.025 and an effective thickness b=0.5 m were assigned to the high-conductive fracture plane. One of the generated realizations was randomly chosen as the reference field. Figure 2 shows the permeability image of the selected reference field. The $^{10}\mathrm{Log}(T)$ mean and variance of the reference field are -2.9908 and 0.169, respectively. The transmissivity at the 8 borehole locations in the reference field honour the actually measured data at the Finnsjön site. The experimental attribute variogram and fitted theoretical variogram model of the reference field are shown in Figure 3. The variogram has an exponential correlation function with a 100 m correlation length, which is also identical to that based on the 8 measurement from the Finnsjön site. The reference field is viewed as a realistic one, reflecting the true field situation.

The north and south horizontal boundaries of the studied domain are assumed to be no flow boundaries, whereas the west and east boundaries are constant with a head of 100 m and 96 m, respectively. These boundary conditions induce a mean flow direction towards to the east boundary with a mean hydraulic gradient of 1/300 which also corresponds to the natural hydraulic gradient measured at the Finnsjön site. The steady state 2D saturated groundwater flow equation with a superimposed dipole test condition was solved using a 5-point standard block centre implicit finite difference scheme with a direct band solver. The injection and pumping rate of the dipole was 7.212 m3/hr at borehole BFI01 and BFI02, respectively, which corresponds to the actual field test conditions. The resultant head distribution and stream line pattern of the reference field are shown in figure 4 and 5, respectively. The tracer is assumed to be injected instantaneously at borehole BFI01 with total mass of 9000 mg (Case 1). The released tracer batch is regarded to be made up of 900 particles with an individual mass of 10 mg. The particles are assumed to be conservative, implying no chemical reactions or sorption during particle transport. The movement of particles is analysed using particle tracking techniques assuming no local dispersion, i.e. only advection is considered. The arrival of particles at borehole BFI02 is recorded as a function of time. Figure 6 shows the breakthrough curve of the reference field. The breakthrough curve has a rapidly rising peak with a long tail which illustrates the marco-dispersion caused by velocity variation and different particle travel paths. A second tracer test was also simulated between borehole KFI11 and BFI02 under prevailing dipole test conditions (Case 2). The same amount of tracer was injected at borehole KFI11 and the resulting breakthrough curve at BFI02 was recorded. The breakthrough curve of the KFI11 test performed in the reference field is shown in Figure 7. Because the distance between KFI11 and BFI02 is much shorter, the breakthrough curve of the KFI11 test has very similar travel times for each particle. The difference in travel time for each particle is caused by the variation in transmissivity. It should be noted that the breakthrough curve of the BFI01 test has shape and time characteristics similar to the actual Finnsjön field dipole test results which again indicates that the selected synthetic reference field well represents the site characteristics and heterogeneity of the Finnsjön site.

The results discussed above are considered to be the real system response of the reference field and should be used for calibration. As indicated previously, in safety assessment of repository performance, radionuclide transport on a larger scale (order of kms) is an important component in the evaluation of the safety of a given repository concept. A groundwater flow and transport model calibrated at a local scale and subsequently extrapolated to a larger scale, also need to be validated at this particular (test) scale. In nature, and under natural, undisturbed conditions, the radionuclide is transported under natural hydraulic gradient conditions, hence a test performed under these more realistic conditions would be a more interesting and relevant demonstration.

In our synthetic reality, the far field simulation was performed under natural gradient conditions. The tracer was instantaneously injected at an area between block (5,26) to (5,35), cf. Figure 2, which covers a 20x200m area. Each block had 1000 mg mass (100 particles) released instantaneously and the breakthrough along the right boundary was recorded. Figure 8 shows the far field simulation breakthrough curve of the reference field. The results show that the breakthrough curve has a very high peak value with a second smaller peak at later time. The particles are dispersed when moving downstream in the model. These far-field simulation results are to be used to validate the overall model, ie. the validity of extrapolating a model calibrated and validated on a local scale to a larger, far-field scale.

4. Simulation of transmissivity fields

Since we know only 8 transmissivity data of the field to be simulated, a greater part of the field will remain uncertain. Estimates of the transmissivity field as obtained by kriging can be used to examine some of the effects of heterogeneity. Since the kriged field has a small variance compared with the sampled data, it does not really reflect the true heterogeneity of the reference field. In order to better understand the effect of heterogeneity, and also to quantify the uncertainty of the solute transport simulation, it is necessary to use a simulation approach. The Monte-Carlo approach is used to generate many equally probable realizations that have the same statistical structure as the measured data. Several methods exist for generating random fields, such as the covariance matrix method (Williams and El-Kadi, 1986), the spectral method (Meija and Rodriguez-Iturbe 1974), and the turning band method (Mantoglou and Wilson, 1982). The turning band method is the most frequently used model in the stochastic continuum approach where the generated fields are approximately Gaussian.

The computer code TUBA (Zimmerman and Wilson, 1990) was used to generate 100 realizations of the studied domain. The ensemble mean and variance of the generated transmissivity fields is -3.2811 and 0.1543, respectively, which should be compared with the corresponding input data (-3.2841, 0.1574). The ensemble correlation structure is an exponential type function with a 100 m correlation length. The generated realizations are inherently unconditional since only the statistical parameters are the same as the measured data whereas the actual transmissivity data at the borehole intercepts with the zone are not honoured. The technique used for subsequent conditioning of the simulations follows that of Delhomme (1979). Figures 9, 10 and 11 show three different transmissivity fields based on the conditional simulation. It may be noted that the ensemble mean transmissivity field of the conditional simulation is the same as the kriged field.

5. Calibration

In simulating the dipole test, steady state 2D groundwater description and instantaneous injection of tracer are used. The 8 measured transmissivity data have been used to infer the transmissivity fields. The remaining undefined parameters are the porosity and effective thickness of the subzone, which need to be calibrated. On the basis of previous work (Andersson et al 1992), a constant porosity, n=0.025 and an effective thickness, b=0.5 m have been used. In the calibration procedure, these two values are chosen as first try values. The flow and transport conditions used when analysing the simulated realizations of transmissivity are identical to those used when analysing the reference field. For each generated flow field, the tracer test was simulated in order to obtain the breakthrough curve at borehole BFI02. Figures 12, 13 and 14 show the calculated head distribution under prevailing dipole test conditions corresponding to the three transmissivity fields in Figures 9, 10 and 11. The stream line patterns of the corresponding transmissivity fields are shown in Figures 15, 16 and 17. Figures 18, 19 and 20 show the corresponding breakthrough curves of the BFI01 test. The breakthrough curve of the KFI11 test of field 2 (Figure 10) and field 3 (Figure 11) are shown in Figure 21 and 22, respectively. It should be noted that for the field 1 simulation, some of the particles injected at borehole KFI11 have not been captured at borehole BFI02, but have moved to the downstream boundary. The results of the different generated fields show different shapes and peak concentrations, and the resulting uncertainty in the results is an effect of heterogeneity.

The ensemble mean head distribution and its variance distribution for the simulated fields are shown in Figures 23 and 24, respectively. Although different realizations have head distributions different from that of the reference field, the ensemble mean head distribution is close to that of the reference field, especially in the region between boreholes BFI01 and BFI02. Figures 25 and 26 show the ensemble breakthrough curve of the two test cases at BFI02 with one standard deviation envelope, respectively. The breakthrough curve of each individual realization is different from the reference field due to uncertainty in transmissivity values. However, the mean (ensemble) breakthrough curve is very close to that of the reference field, and the envelope shows the uncertainty of the simulation. The simulation of the BFI01 test (Figure 25) is better performed than that of the KFI11 test (Figure 26).

Calibration of a stochastic model is a less clear a process than that of calibrating a deterministic model, since the predictions of the former type of models are associated with inherent uncertainty. The input statistical properties of a given field are estimated from sampling data. Due to the limited number of sampling data and associated sampling error, these statistical properties can be biased, e.g., mean and variance may deviate from the true values, reflected in this case by the fact that the sampling data have mean and variance different from the reference field. The correlation function and its integral scale are estimated from variogram analysis which can also be biased. In practical simulation, these statistical parameters also need to be calibrated by using field data such as groundwater head, tracer breakthrough curves, etc., after the simulation results are available. In this study, we do not intend to calibrate the statistical parameters which are used in the model. The reason for choosing this approach is that in a practical situation we usually lack data to do the cross-validation of the transmissivity, ie. all data are used in the statistical analysis. Instead, we have concentrated on the calibration of the assumed constant parameters in the model, ie., porosity and effective thickness of the subhorizontal subzone.

In general, the porosity and effective thickness are not constant in the formation. In practice, the porosity and effective thickness are estimated from few sampling points or estimated by expert judgement. It is plausible to assume that porosity and effective thickness have much longer correlation lengths and smaller variation than the transmissivity. In most situations, the porosity and the effective thickness are assumed to be constant in the model. If they are constant in the model, porosity and effective thickness have the same influence on particle transport as changing the velocity by a constant rate. Under this assumption, we only have one parameter to be estimated in the model. For example, a porosity increase by 20% implies that the velocity will be reduced to 83% and the particles mean arrival time will be increased by 20%.

The breakthrough curve of the simulated KFI11 test (Case 2) has an earlier (first) arrival time than that based on the reference case. On the basis of this information we increased the porosity to $n=0.03$ for the second try. The resulting ensemble breakthrough curve of the two test cases at BFI02 together with one standard deviation envelope are shown in Figures 27 and 28, respectively. The results show that the arrival time of the BFI01 test is later than that of the reference field due to velocities being slowed down along the dipole path lines. The breakthrough curve for the KFI11 test is closer to the reference field results than the previous simulation results with $n=0.025$, but with somewhat increased dispersion phenomena. This implies either that the generated transmissivity between KFI11 and BFI02 is possibly higher than in the reference field, or that its porosity should be higher. It should be noted that calibration of parameters in order to obtain the best fit of measured breakthrough curve results does not guarantee that the correct parameters will be obtained. For example, one can reduce porosity between borehole KFI11 and BFI02 to get best fit solution, but actually the porosity used in the reference field is constant in the whole domain. The same situation applies for the effective thickness of the subzone. Calibration utilizing limited data and information is largely subjective. Based on the simulation results, we concluded that a porosity n=0.025 and an effective thickness b=0.5 m are the most suitable model parameters. It is worth noting that both test cases have similar transport length scales, and being subject to the same test conditions which only represent part of the response of the field.

Another approach to calibration of the parameters is to compare each breakthrough curve of the simulated fields with the reference field to sort out the transmissivity field which best fits the reference field breakthrough curve. The suggested criterion for selection of the best fitted curve is to quantify the deviation of the simulated breakthrough curve from that of the reference field. The index of deviation (ID) is calculated using the following formula;

$$ID = \text{sum}((C_s - C_r)^2)/\text{number of time intervals}$$

where C_s and C_r are values of concentration of the breakthrough curves of the simulated and reference field, respectively. The ID of each realization are listed in Table 2. In the table, the index of deviation of the KFI11 test case is indicated only for the realizations which has a lower index of deviation for the BFI01 test case. From Table 2, we can distinguish three fields (#22, 38 and 96) which, according to there index of deviation, are best suited for calibration. The field with the best fit is field #22. The mean and variance of transmissivity of these fields together with the corresponding statistics of the reference field and sampled data are shown in Table 1.

The breakthrough curve of the two test cases (BFI01 and KFI11) of field #22 together with the corresponding reference case results are shown in Figures 29 and 30, respectively. Figure 31, 32, 33 and 34 show the corresponding breakthrough curves of the fields #38 and 96, respectively. Based on the statistical parameters and index of deviation of the breakthrough curve, we concluded that field #22 is the best calibrated one. This approach of calibration resembles that used when applying the deterministic calibration approach.

6. Validation on a larger scale

We discuss here the validation of a stochastic continuum model calibrated on a local scale, for predicting far-field scale (test) responses, the latter substantiated by comparison with reference field results. If the simulated far-field results are close to the reference case, we say that the model is validated.

The far-field simulations were calculated under natural gradient conditions using the same transmissivity fields as for the local scale dipole test. The tracer was injected in accordance with the reference case analysis. Figures 35, 36 and 37 show three different far-field breakthrough curves corresponding to different transmissivity fields, c.f. Figure 8. The results show very different mean arrival times and dispersion patterns. Figure 38 shows the resulting ensemble breakthrough curve for the far-field simulation. The results show essentially none of the charcteristics of the far-field simulation based on the reference field, this since the transmissivity is known only at 8 points representing the local test scale only. This result shows that calibration of the model on the local scale (which is often less heterogeneous) and subsequent prediction of far-field transport phenomena can result in erronenous results, i.e. the model calibrated on a local scale is insufficient to validate the large scale simulation.

Adding more measurement data and conditioning on them can however improve the simulation. To demonstrate the effect of the number of conditioning data on the simulation results, 28 new point were randomly selected on a far-field scale from the reference field forming new measurement data. Thus, a total of 36 measurement points (1%) were used for new conditional simulations of the same dipole test cases and far field simulation. Figure 39 shows the new measurement locations. The ensemble mean breakthrough curve of the two test cases at BFI02 are shown in Figures 40 and 41, respectively. Figure 42 shows the resulting ensemble breakthrough curve of the far field simulation by using 36 conditioning points. The calculation results on the local (dipole test) scale are similar to the results obtained when using only 8 conditioning points. In this situation, adding more measurement points on a larger scale does not improve the quality in the simulations on a local scale. In terms of the far-field simulation, where transport length scale is much longer than the local scale, the simulation results are improved by the added conditioning points. The resulting breakthrough curve is more compressed and the peak values shifted towards the correct time interval, c.f. Figure 8, as compared to the results based on 8 point conditioning.

Figure 43, 44 and 45 show the breakthrough curves of the far field simulations based on fields #22, 38 and 96, respectively. The breakthrough curves of these 3 best fitted fields are quite different from each other and different from reference field results. The breakthrough curve of field #38 is similar in shape to the reference field but with a much longer travel time. Based on the far field simulation, it can be stated that field #22 is not validated, despite its local scale calibration. Field #38 can be said to exhibit some degree of validation.

7. Discussion of results

We have demonstrated two ways of calibration, one being calibration with a model's statistical parameters and its assumed constant parameters (ie. porosity and effective thickness), the other being calibration to a particular field with same statistical characteristics.

The first approach shows that calibration on a local scale is insufficient to provide acceptable model predictions on a large scale. The uncertainty in large scale prediction cannot be reduced when only limited amount of data are available. More sampling data can improve the quality of the simulation. The second approach resembles the classical deterministic approach to calibration. However, the results of validation show that the best fitted calibrated field on a local scale does not turn out to be validated on the larger scale. This again shows that calibration on a local scale is insufficient to validate the model on a large scale. Although, field #38 has a breakthrough curve of far-field simulation similar to the reference field, we believe that this is simply by chance, sometimes it can be quite different compared to the reference field as in the case of fields #22 and #96. The stochastic feature of a given field is lost when calibration is made with this deterministic approach. The statistical parameters are used for constructing a heterogeneous field which has the same statistical characteristics as the sampled data. If one assumes that the calibrated and validated field can represent a given domain, the predictions based on this validated field are deterministic and the uncertainty information of the prediction is lost. In addition, in most situations, the particular field is very difficult to identify based on limited amount of measured data.

In reality, we do not have access to the exhaustive information about the transmissivity field we are studying. We only know the system response in parts of the field. It is more preferable to have tests which cover more area (volume) of a given field and with longer duration. Calibration and validation are more difficult in the actual field situation with only limited amount of measured data, and thus the calibration and validation process still remain more subjective than objective.

The results of this study show that tracer tests on a scale of about 200m can successfully be used to calibrate and validate performance assessment models on a corresponding scale. This implies that these types of tests could be used to calibrate and validate performance assessment models that describe a compartment of near-field rock either 1) along a storage tunnel including some 30 potential canister deposition hole locations, or 2) transecting a repository perpendicular to the storage tunnels covering some 8-9 tunnels at an arbitrary position. They could also be used to study the transission zone between near- and far-field models. This scale would correspond to defined safety distances between the repository perimeter and the closest defined Local Fracture Zone.

The use of large scale multi-borehole tests to improve near-field performance assessment models will be governed by 1) performance criteria set by the licenseé and by the licensing body, 2) availability of boreholes of suitable geometry, and 3) time constraints in the repository production. Obviously, there exists no urge to turn the potential repository environment into a "Swiss cheese" by extensive drilling which might breech the containing ability of the rock. Hence, ample use must be made of existing or planned necessary boreholes, eg. pilot holes for storage tunnels. Permanent installations could also be used to monitor the repository performance over time.

8. Conclusions

A realistic synthetic transmissivity field and dipole test conditions similar to the actual field tests at Finnsjön were used to demonstrate the calibration and validation procedure applied to a stochastic continuum model. The results show that calibration on a local scale is insufficient for validating the model on another larger transport scale.

Simulation using the stochastic continuum approach is always associated with uncertainty. Calibration of this type of model is better performed using statistical approaches rather than deterministically. In the latter case the identification of a particular "best fit" realization of transmissivity field is a difficult task, which in addition results in a loss of uncertainty by the added increase of its deterministic strength.

We believe that calibration and validation of stochastic continuum model still remain more subjective than objective, and perhaps the work of Luis and McLaughlin (1991) and Ababou et al (1992) can provide means of making this process less subjective. The confidence in the prediction results depends on the information that is collected from a given field and the degree of confidence in the model structure.

More measurement data on relevant scales can reduce the uncertainty of the simulation. In practice, one should first identify the scale of the problem of interest and perform testing and measurements in accordance with the selected scale. A natural gradient tracer test at a larger scale is an ideal validation exercise which, however, may be practically unfeasible. In that case a number of tracer tests at a smaller scale, distributed over the flow domain of interest, may be an acceptable compromise to inform and piecewise validate the performance assessment.

9. References

Ababou, R., Sagar, B. and Wittmeyer, G. 1992 : Testing procedure for Spatially Distributed Flow Models. Adv. Water Res., vol. 2 of special issue on model validation, 1992.

Andersson, P. and co-workers 1992 : SGAB/SKB Analysis of Hydrologic and Tracer Data. In Tsang, C-F. and Neuman, S. ed:s, Phase 1, Test Case 5, Studies of Tracer Experiments in a Fracture Zone at the Finnsjön Research Area. The International INTRAVAL Project, OECD/NEA/SKI, Paris.

Cliffe, K.A., Jackson, C.P. and Impey, M.D. (in prep.) : A Preliminary Study of the WIPP2 Test Case. AEA/NSS Report, U.K.

Davis, P.A. and Goodrich, M.T. 1990 : A proposed Strategy for the Validation of Ground-water Flow and Solute Transport Models. In Proc. of the GEOVAL-90 symposium on validation of geosphere flow and transport models. SKI and OECD/NEA, Stockholm.

Delhomme, J.P. 1979 : Spatial Variability and Uncertainty in Groundwater Flow Parameters : A geostatistical Approach. Water Resour. Res., vol. 15, no. 2, pp. 269-280.

Goblet, P. 1992 : EMP Analysis of Tracer Data. In Tsang, C-F. and Neuman, S. ed:s, Phase 1, Test Case 5, Studies of Tracer Experiments in a Fracture Zone at the Finnsjön Research Area. The International INTRAVAL Project, OECD/NEA/SKI, Paris.

Grindrod, P. and Capon, P. 1991 : Flow through Fractured Rock : What does the WIPP Site Culebra Data Reveal? Unpublished internal INTERA report, Intera, UK.

Grindrod, P. and Worth, D.J. 1992 : Intera Analysis of Tracer Data. In Tsang, C-F. and Neuman, S. ed:s, Phase 1, Test Case 5, Studies of Tracer Experiments in a Fracture Zone at the Finnsjön Research Area. The International INTRAVAL Project, OECD/NEA/SKI, Paris.

Hautojärvi, A. and co-workers 1992 : VTT Analysis of Tracer Test Data. In Tsang, C-F. and Neuman, S. ed:s, Phase 1, Test Case 5, Studies of Tracer Experiments in a Fracture Zone at the Finnsjön Research Area. The International INTRAVAL Project, OECD/NEA/SKI, Paris.

Kimura, H. and Manukata, M. 1992 : JAERI Analysis of Tracer Test Data. In Tsang, C-F. and Neuman, S. ed:s, Phase 1, Test Case 5, Studies of Tracer Experiments in a Fracture Zone at the Finnsjön Research Area. The International INTRAVAL Project, OECD/NEA/SKI, Paris.

Luis, S. and McLaughlin, D. 1992 : A Stochastic Approach to Model Validation. Adv. Water Res., vol. 1 of special issue on model validation, 1992.

Mantoglou, A. and Wilson, J.L. 1982 : The Turning Bands Method for Simulation of Random Fields Using Line Generation by a Spectral Method. Water Resour. Res., vol. 18, no. 5, pp. 1379-1394.

Meija, J.M. and Rodriguez-Iturbe, I. 1974 : On the Synthesis of Random Field Sampling from the Spectrum : An Application to the Generation of Hydraulic Spatial Processes. Water Resour. Res., vol. 10, no. 4, pp. 705-715.

Moreno. L. and Neretnieks, I. 1992 : KTH/SKB Analysis of the Radially Convergent Experiment. In Tsang, C-F. and Neuman, S. ed:s, Phase 1, Test Case 5, Studies of Tracer Experiments in a Fracture Zone at the Finnsjön Research Area. The International INTRAVAL Project, OECD/NEA/SKI, Paris.

Neuman, S.P. 1992 : Validation of Safety Assessment Models as a Process of Scientific and Public Confidence Building. In : Proc. 1992 Int. High Level Radioactive Waste Conf., April 12-16, Las Vegas, NV.

Sargent, R.G. 1984 : Simulation Model Validation. Simulation and Model-based Methodologies : An Integrate View. Edited by Oren et al, Springer-Verlag, Berlin.

Tsang, C-F. 1991 : The Modelling Process and Model Validation. Groundwater, vol.29, no. 6, pp. 825-831.

Williams, S.A. and El-Kadi, A.I. 1986 : COVAR - A Computer Program for Generat ing Two-dimensional Fields of Auto-correlated Parameters by Matrix Decomposition. Int. Groundwater Modelling Center, Holcomb Res. Inst., Butler Univ, Indianapolis, IND.

Yamashita, R. and Kobayashi, A. 1992 : HAZAMA Analysis of Tracer Test Data. In Tsang, C-F. and Neuman, S. ed:s, Phase 1, Test Case 5, Studies of Tracer Experiments in a Fracture Zone at the Finnsjön Research Area. The International INTRAVAL Project, OECD/NEA/SKI, Paris.

Zimmerman, D.A. and Wilson, J.L. 1990 : Description of and User's Manual for TUBA : A Computer Code for Generating Two-dimensional Random Fields via Turning Bands Method. SeaSoft, Scientific & Engineering Analysis Software, NM.

Table 1 **Statistics of $^{10}\log T$ (m^2/s) for different analysed transmissivity fields.**

Population	Mean	Variance	No. of data
Reference field	-2.9909	0.1690	3600
Field data	-3.2841	0.1574	8
Ensemble	-3.2811	0.1543	100 realizations
Field 22	-3.5030	0.1336	3600
Field 38	-3.0261	0.1656	3600
Field 96	-3.4130	0.1534	3600

Table 2 Index of deviation (ID) between simulated fields and the reference field for the two simulated tracer test cases; Case 1 (BFI01) and Case 2 (KFI11). No entry for Case 2 implies ID(Case1)>ID(Case2).

No.	BFI01	KFI11	No.	BFI01	KFI11	No.	BFI02	KFI11
1	2451.5		35	337.4	4176.4	69	1640.2	
2	1565.5		36	2219.0		70	959.0	
3	490.2	3570.8	37	2246.5		71	3456.9	
4	700.8	4176.4	38	725.6	599.3	72	361.3	2607.3
5	2355.0		39	1321.6		73	1621.7	
6	2477.6		40	620.8	8767.6	74	460.0	3345.7
7	215.0	6949.9	41	1187.0		75	1477.2	
8	1018.0		42	1813.7		76	1681.1	
9	880.8		43	2329.3		77	181.6	15211.9
10	2003.6		44	1027.2		78	2315.7	
11	200.3	3663.8	45	2647.5		79	1716.5	
12	1509.3		46	1456.6		80	1394.5	
13	2272.7		47	345.9	4176.4	81	1756.4	
14	2013.3		48	290.4	12762.7	82	202.3	13636.1
15	2372.3		49	1071.5		83	1440.1	
16	329.6	13818.3	50	1515.7		84	1320.5	
17	528.7		51	2579.4		85	3136.5	
18	2039.7		52	652.0	2656.1	86	2143.1	
19	2208.5		53	1502.5		87	2486.3	
20	2783.9		54	2987.1		88	1087.0	
21	3063.8		55	2093.7		89	5243.3	
22	224.6	332.1	56	710.5	8612.7	90	1171.4	
23	403.7	5482.7	57	2383.6		91	307.7	3856.0
24	750.1	5353.8	58	2634.7		92	2944.6	
25	1975.6		59	2726.8		93	1378.6	
26	154.2	5614.4	60	644.1	8242.2	94	639.5	3353.8
27	1436.3		61	1274.0		95	3769.1	
28	1195.0		62	449.7	3005.8	96	424.3	538.6
29	2409.0		63	4050.9		97	1645.5	
30	1811.0		64	414.5	5349.7	98	3317.9	
31	2205.5		65	1791.4		99	2126.9	
32	1604.9		66	415.5	4170.1	100	276.7	10017.4
33	377.8	4494.1	67	2138.7				
34	1252.4		68	1965.2				

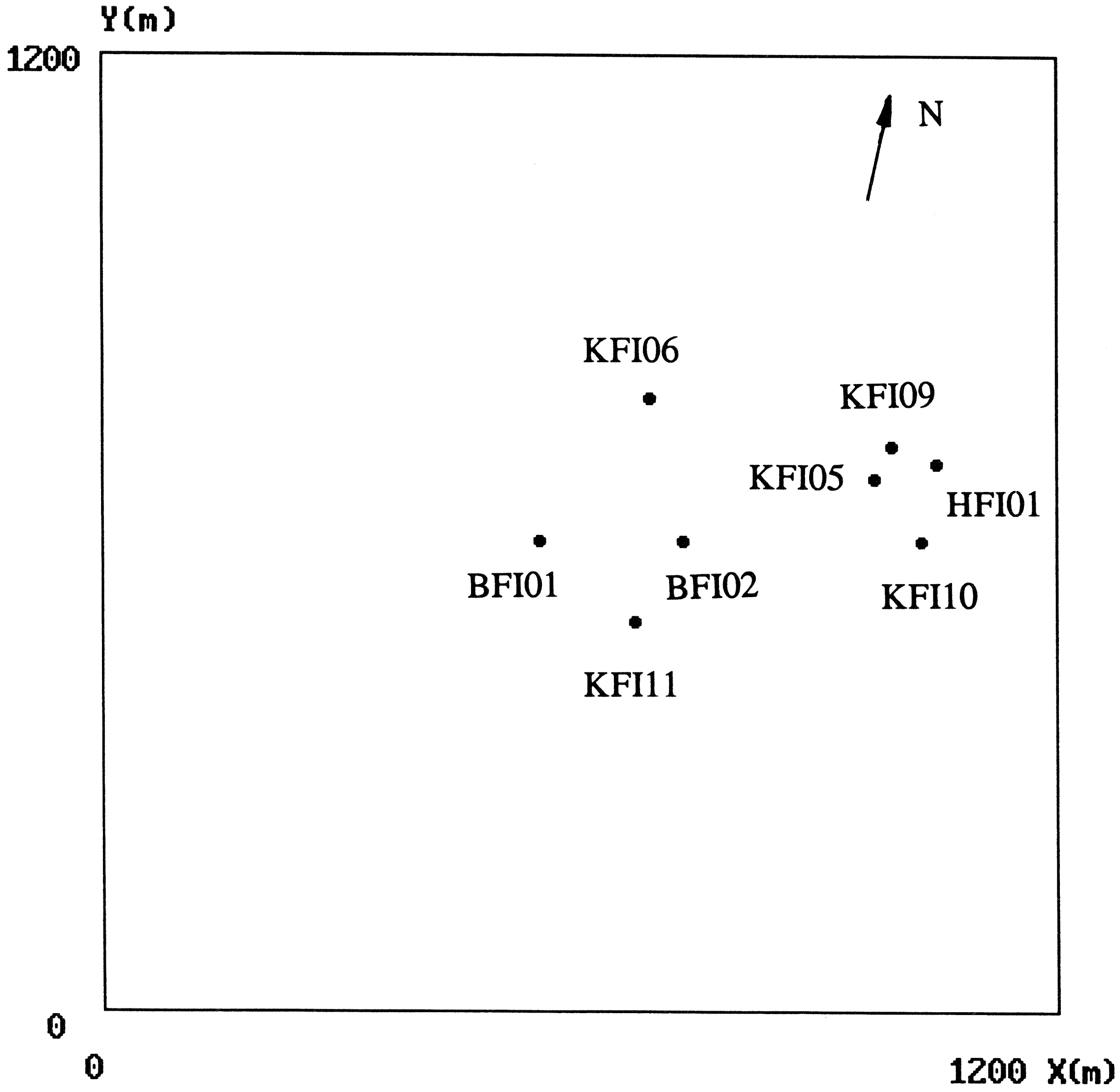

Figure 1 The sampling borehole locations

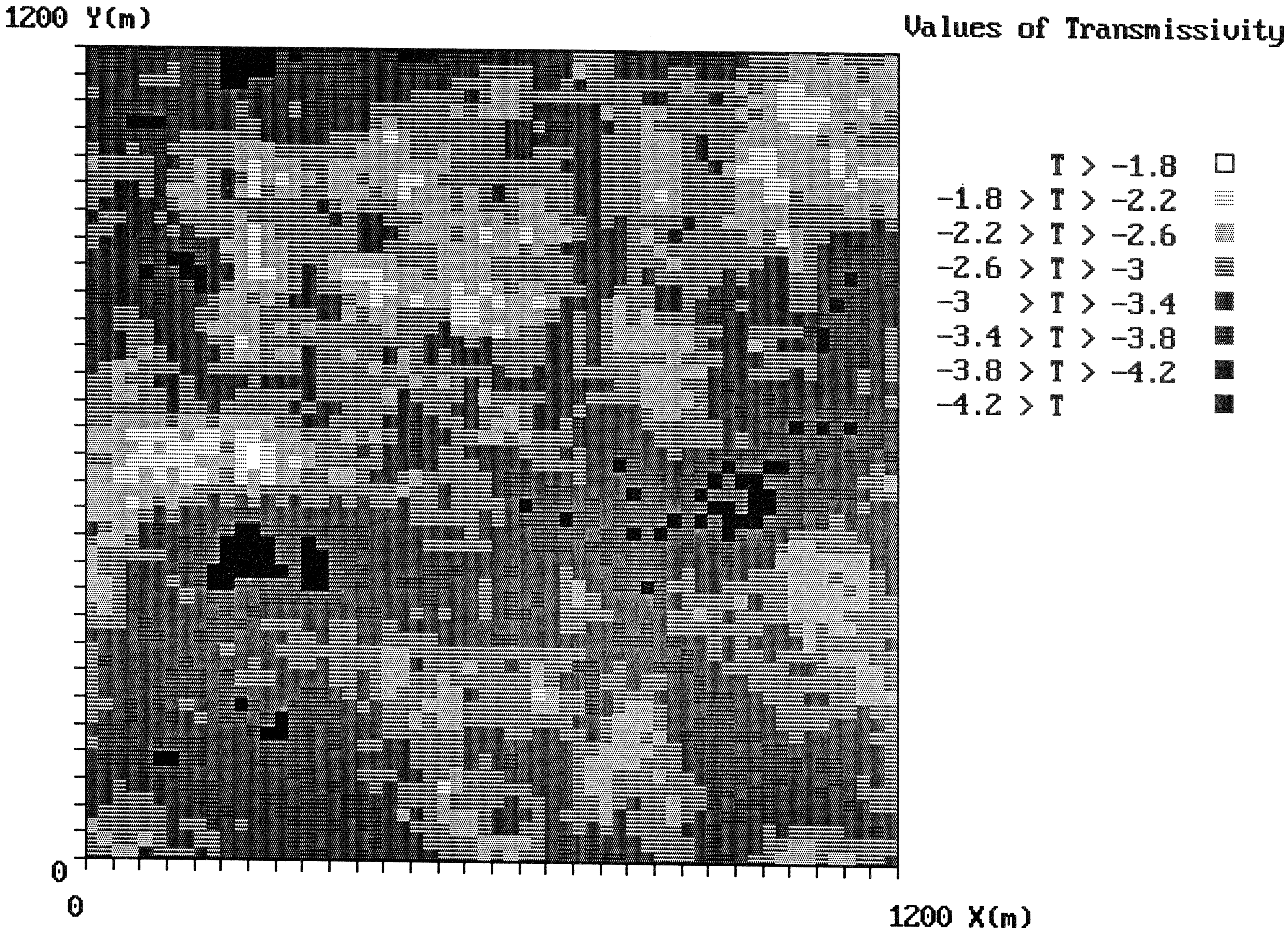

Figure 2 Transmissivity image of the reference field

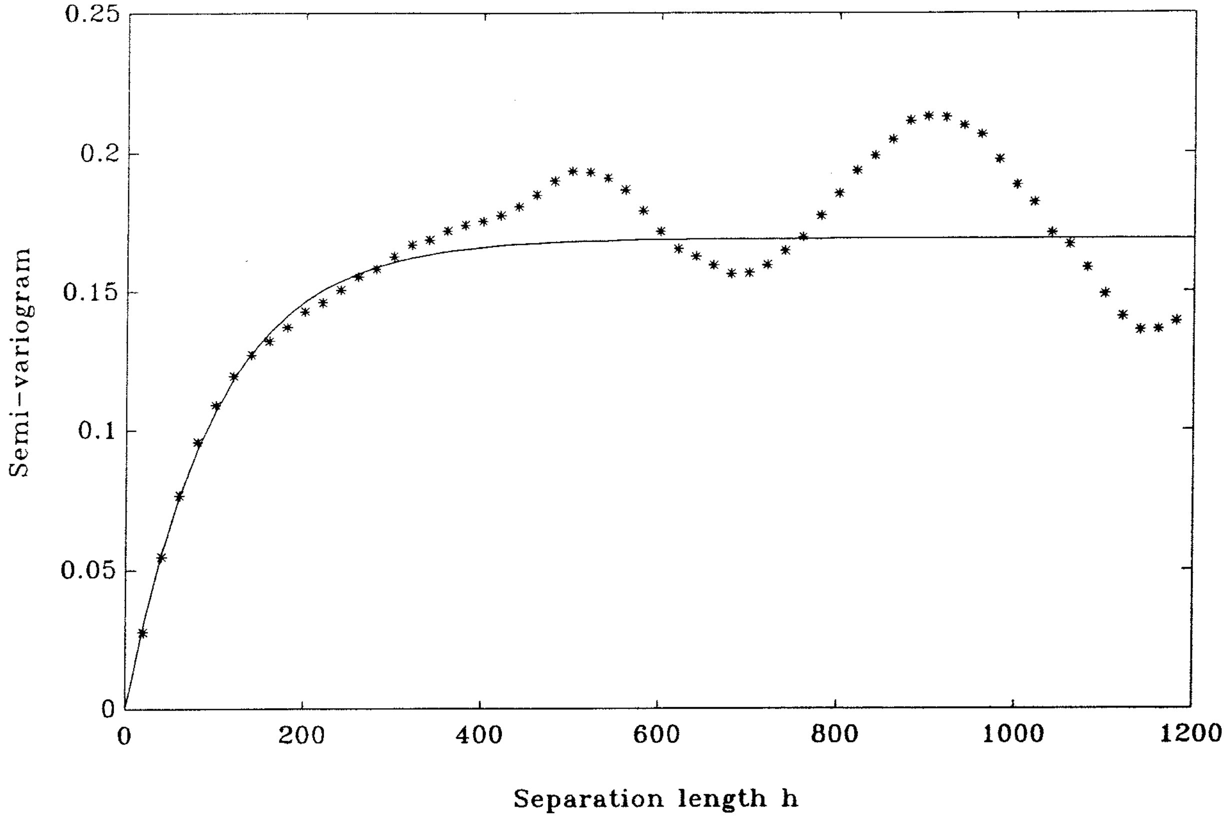

Figure 3 Experimental and fitted theoretical variogram of the reference field

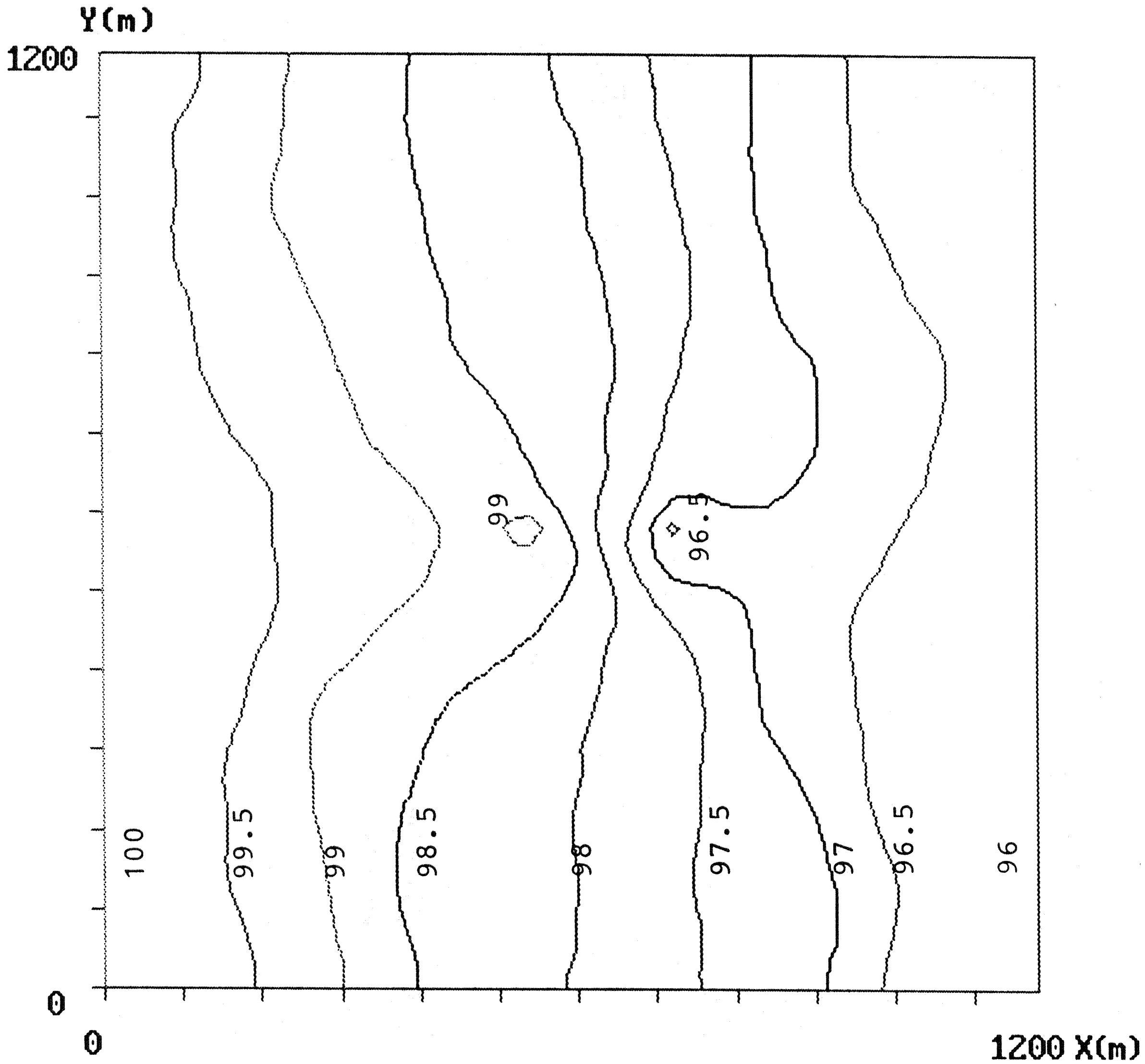

Figure 4 Head distribution calculated from the reference field

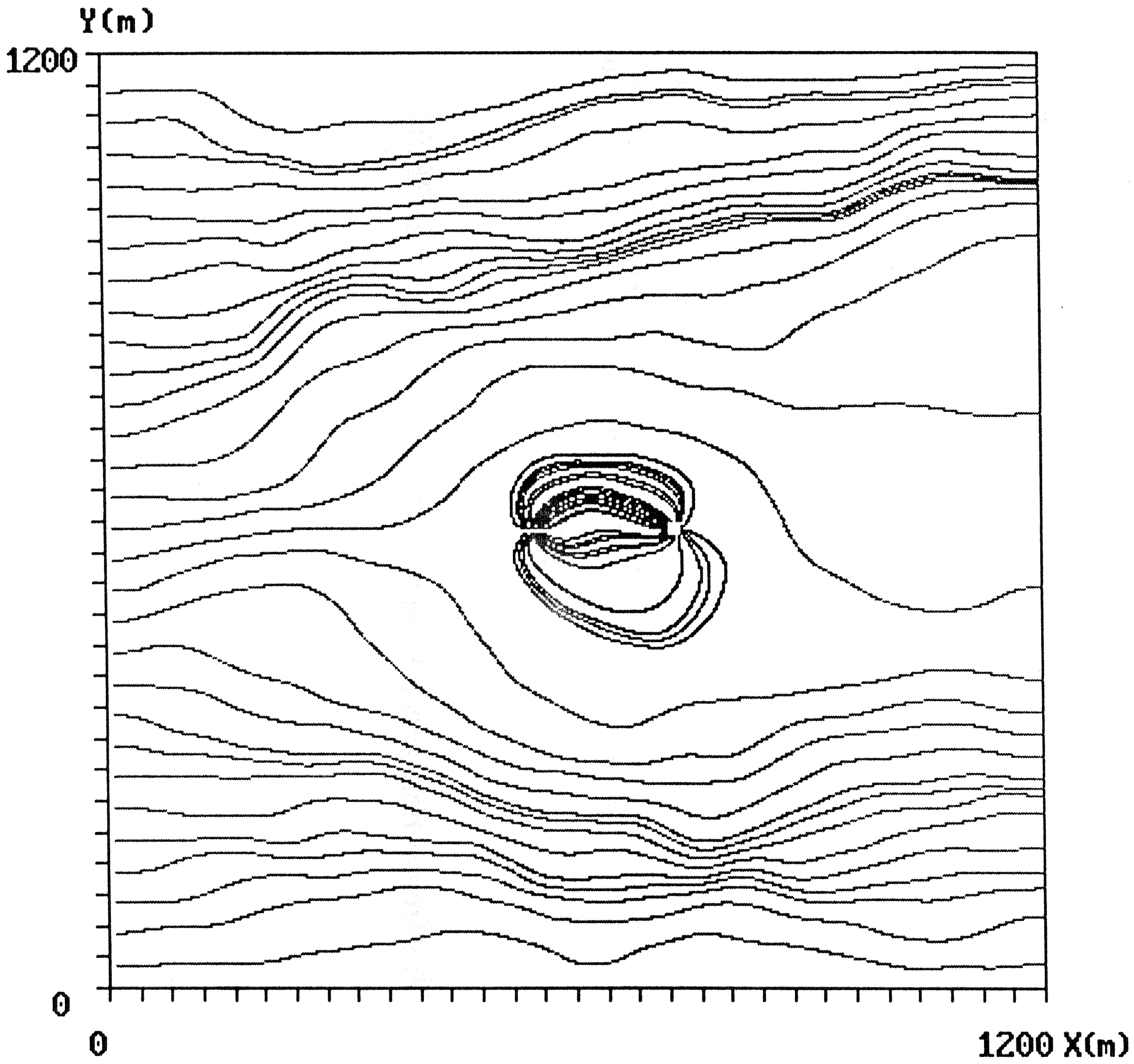

Figure 5 Streamline pattern calculated from the reference field

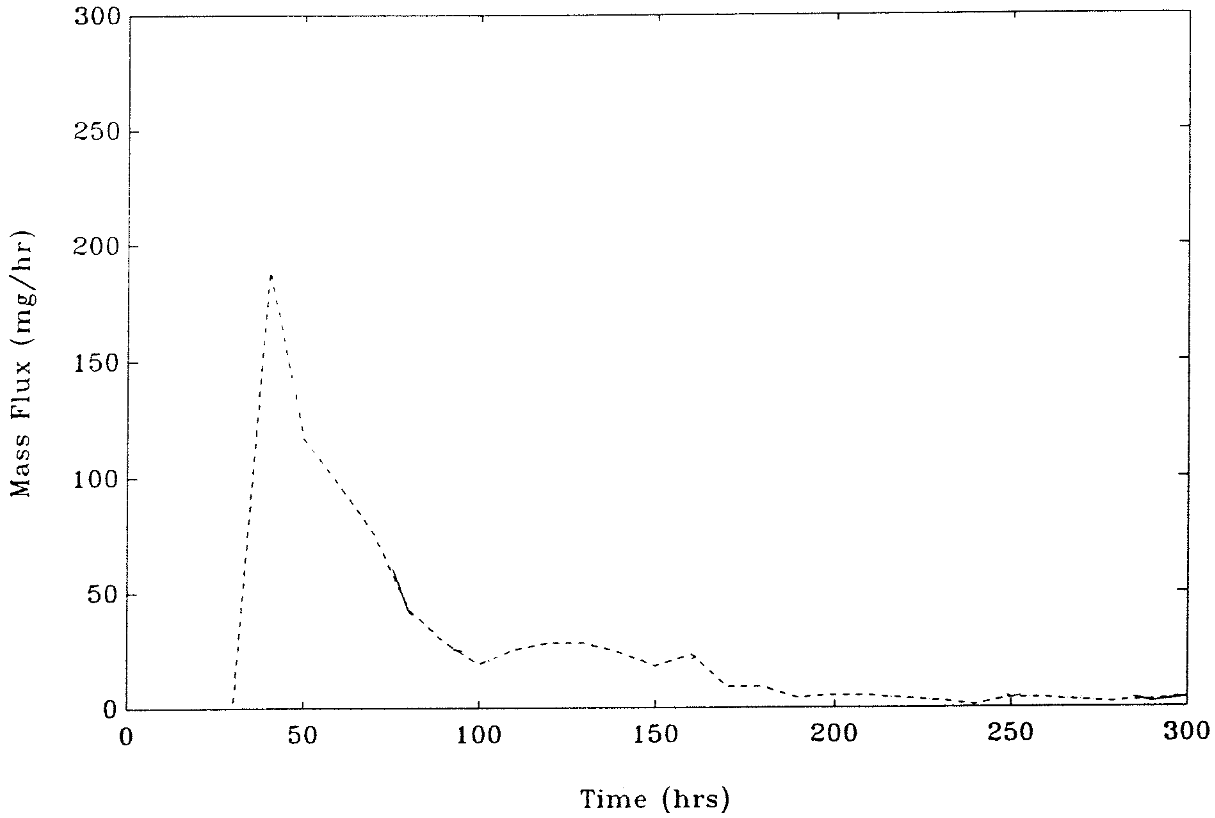

Figure 6 Reference field breakthrough curve for Case 1 test at BFI02

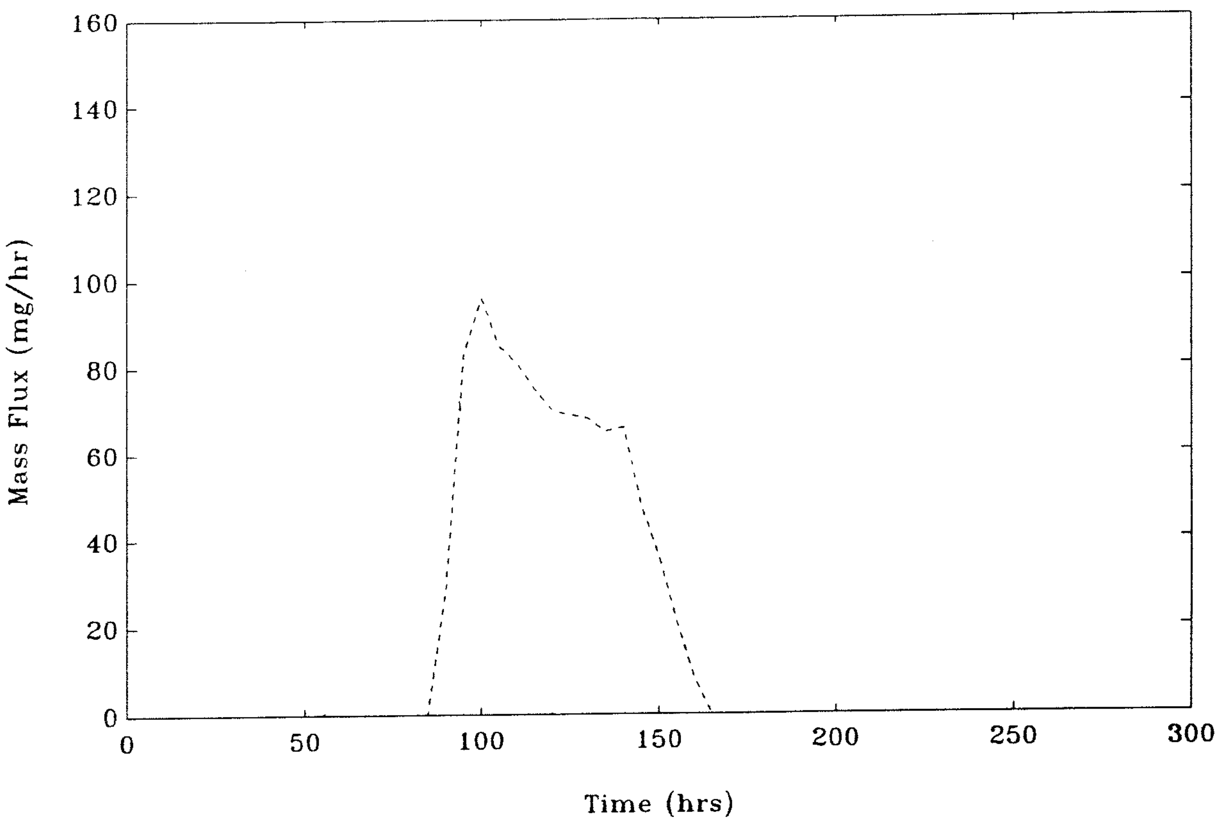

Figure 7 Reference field breakthrough curve for Case 2 test at BFI02

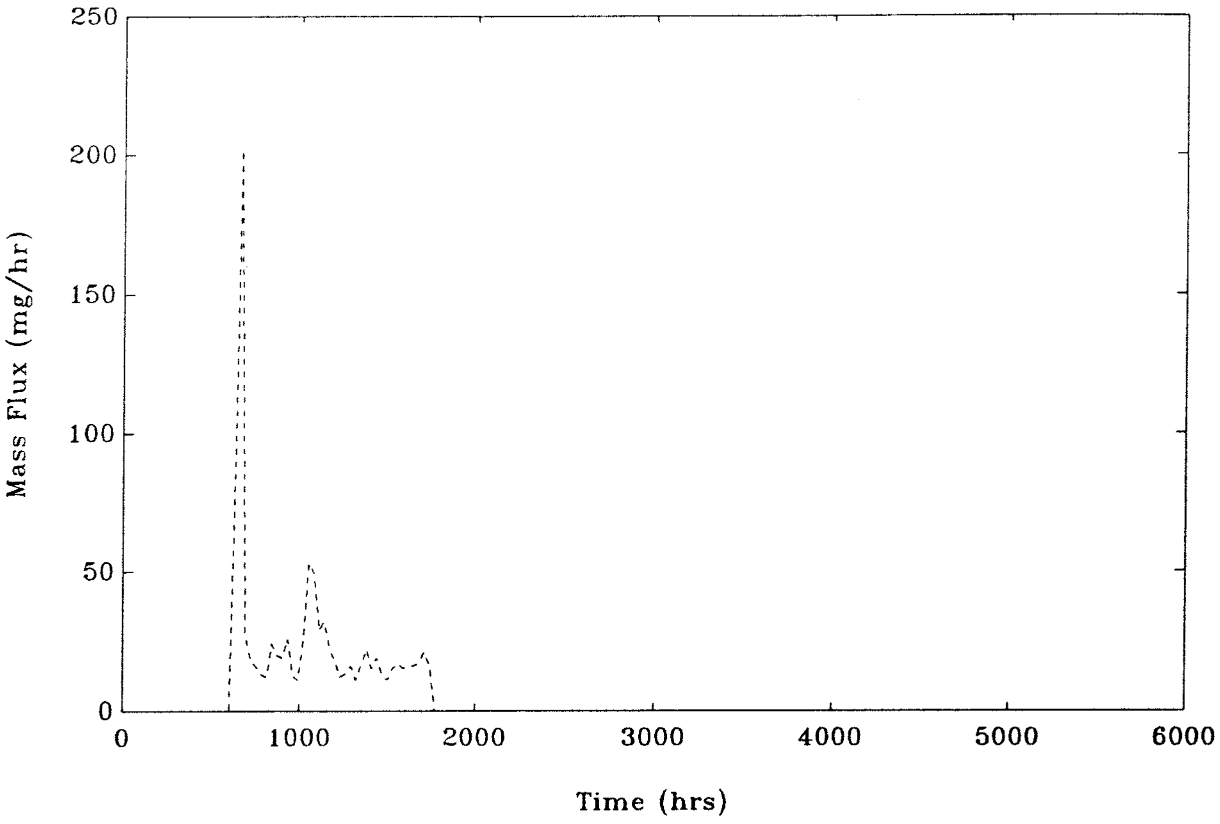

Figure 8 Reference field breakthrough curve for far field simulation

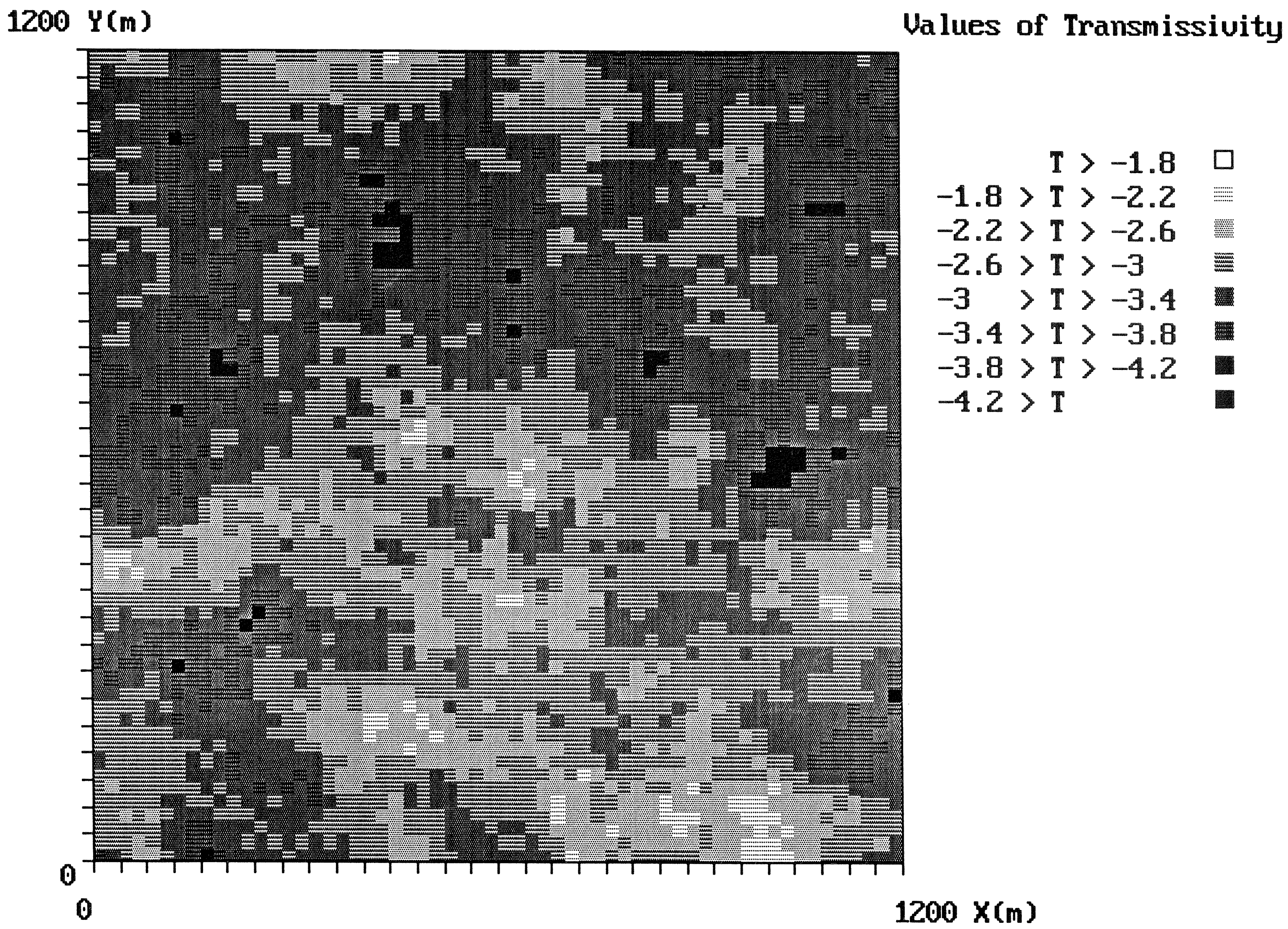

Figure 9 Transmissivity image of conditional simulation (Field 1)

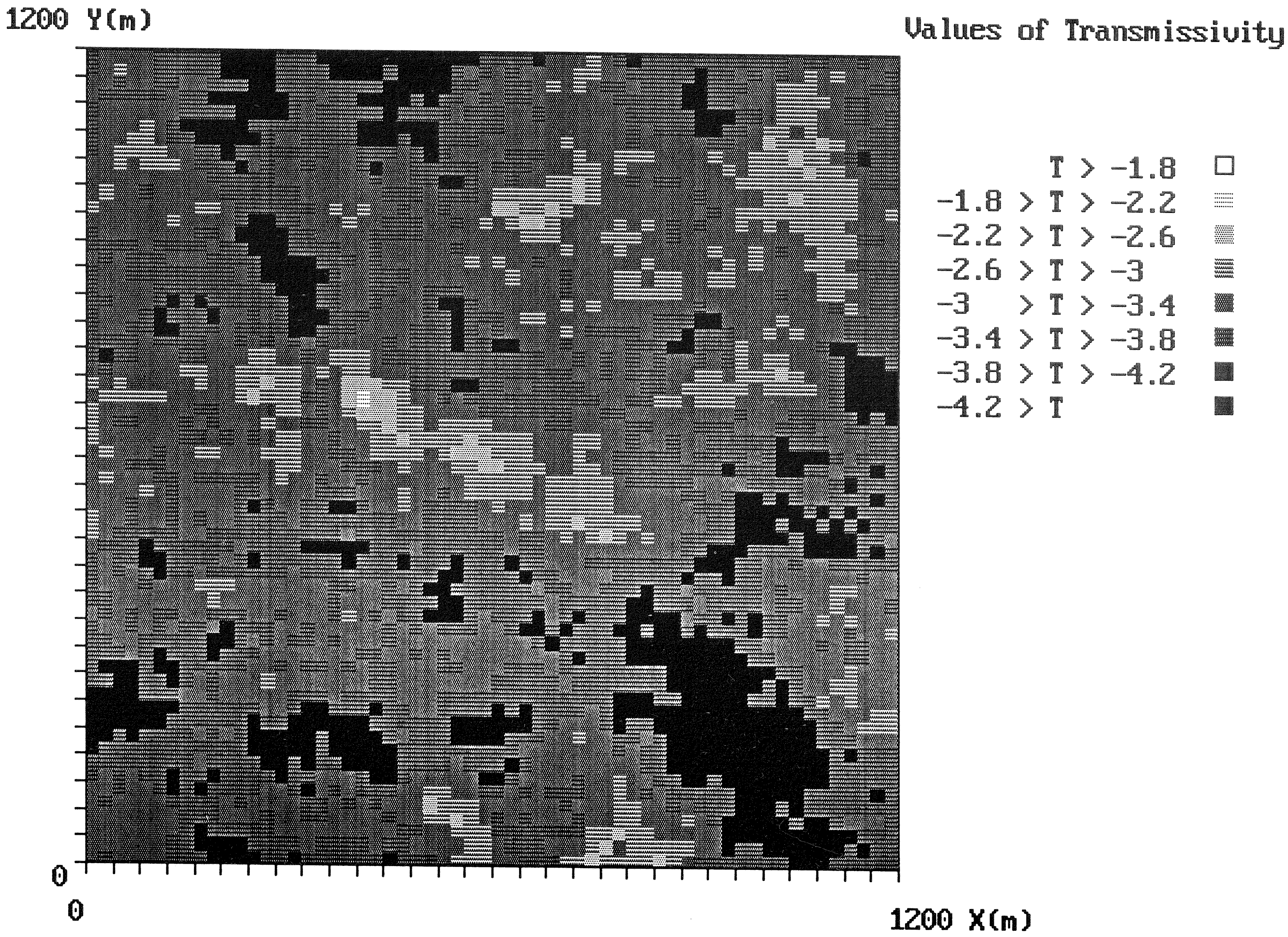

Figure 10 Transmissivity image of conditional simulation (Field 2)

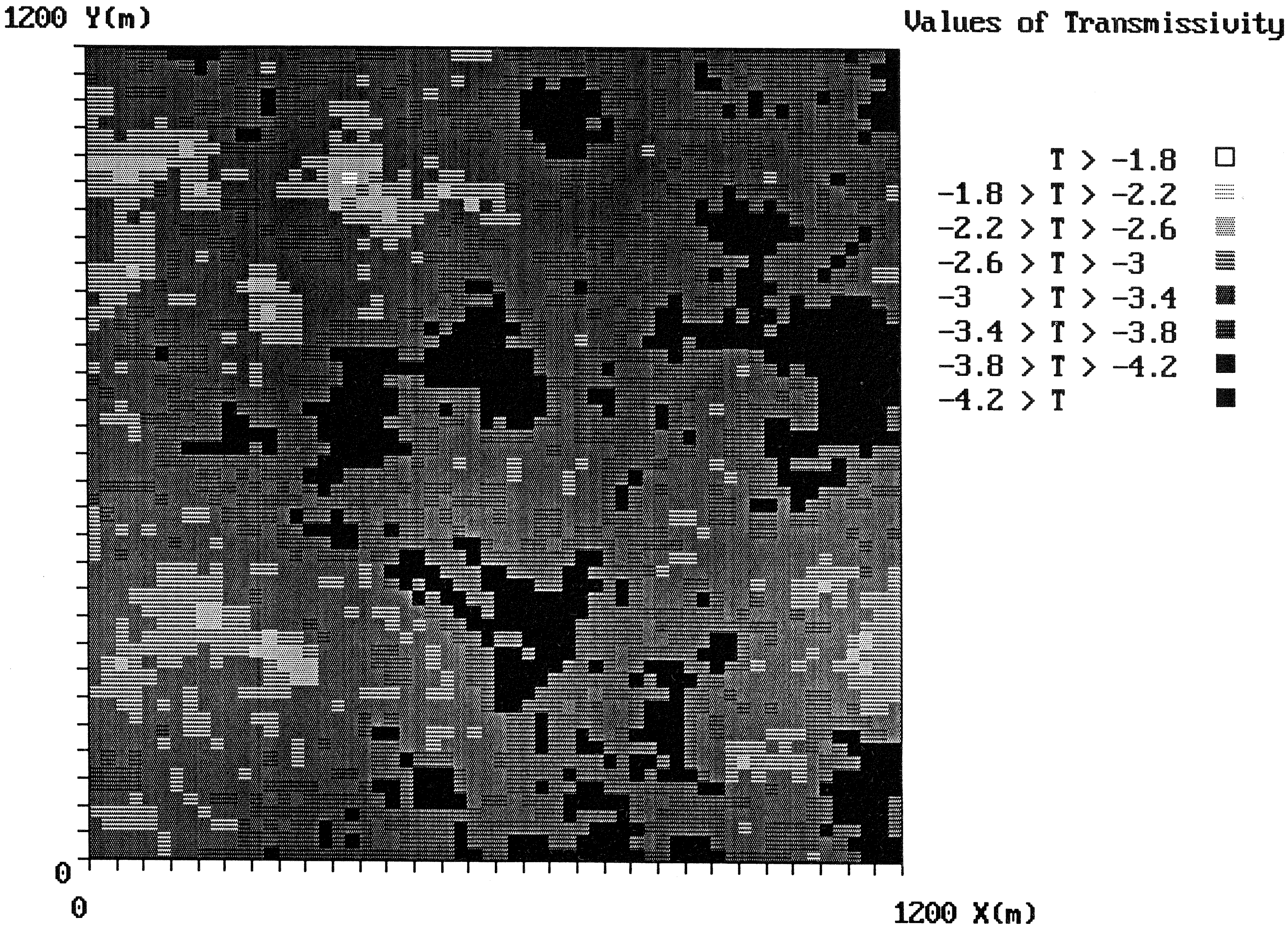

Figure 11 Transmissivity image of conditional simulation (Field 3)

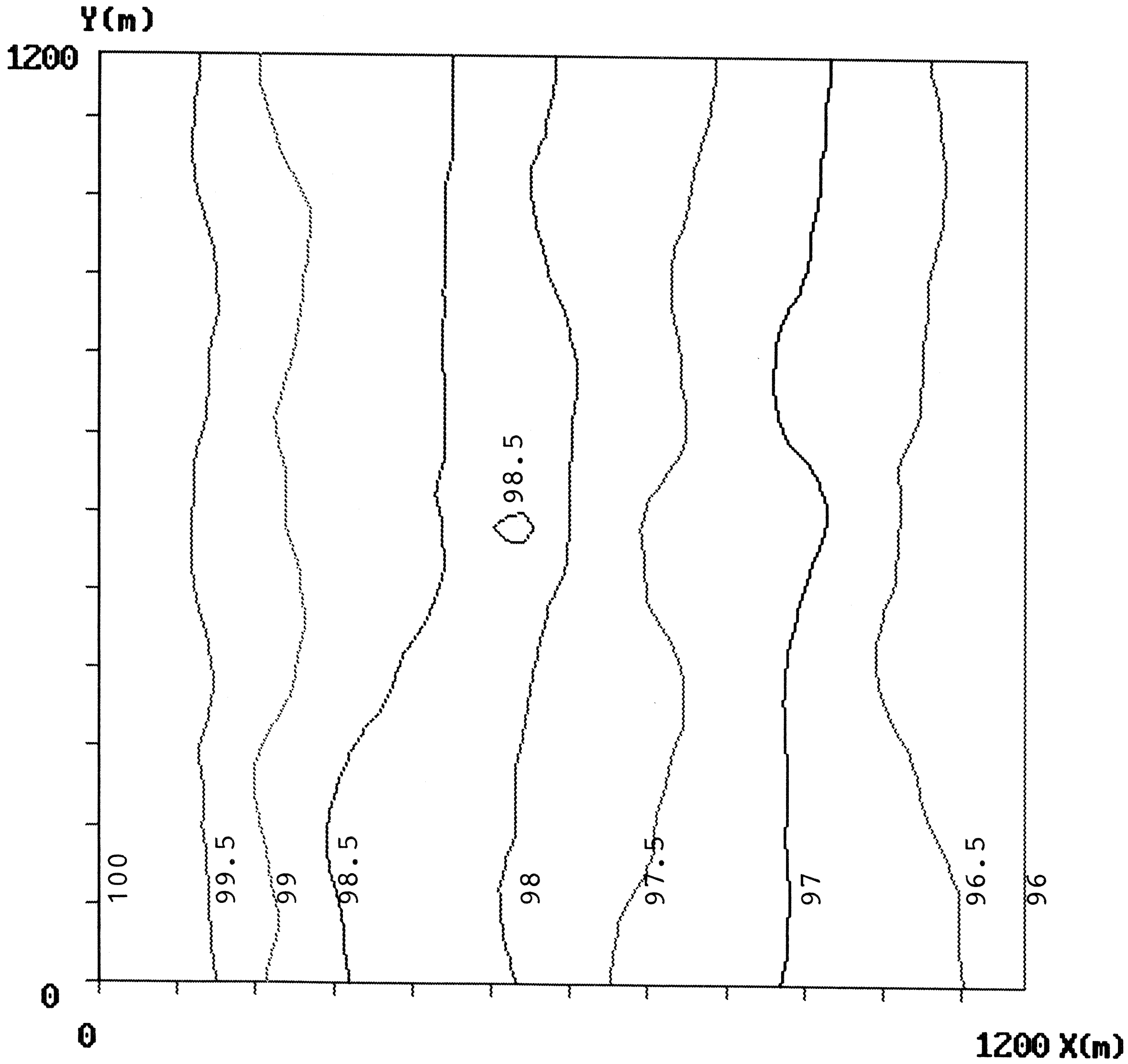

Figure 12   Head distribution calculated from field 1

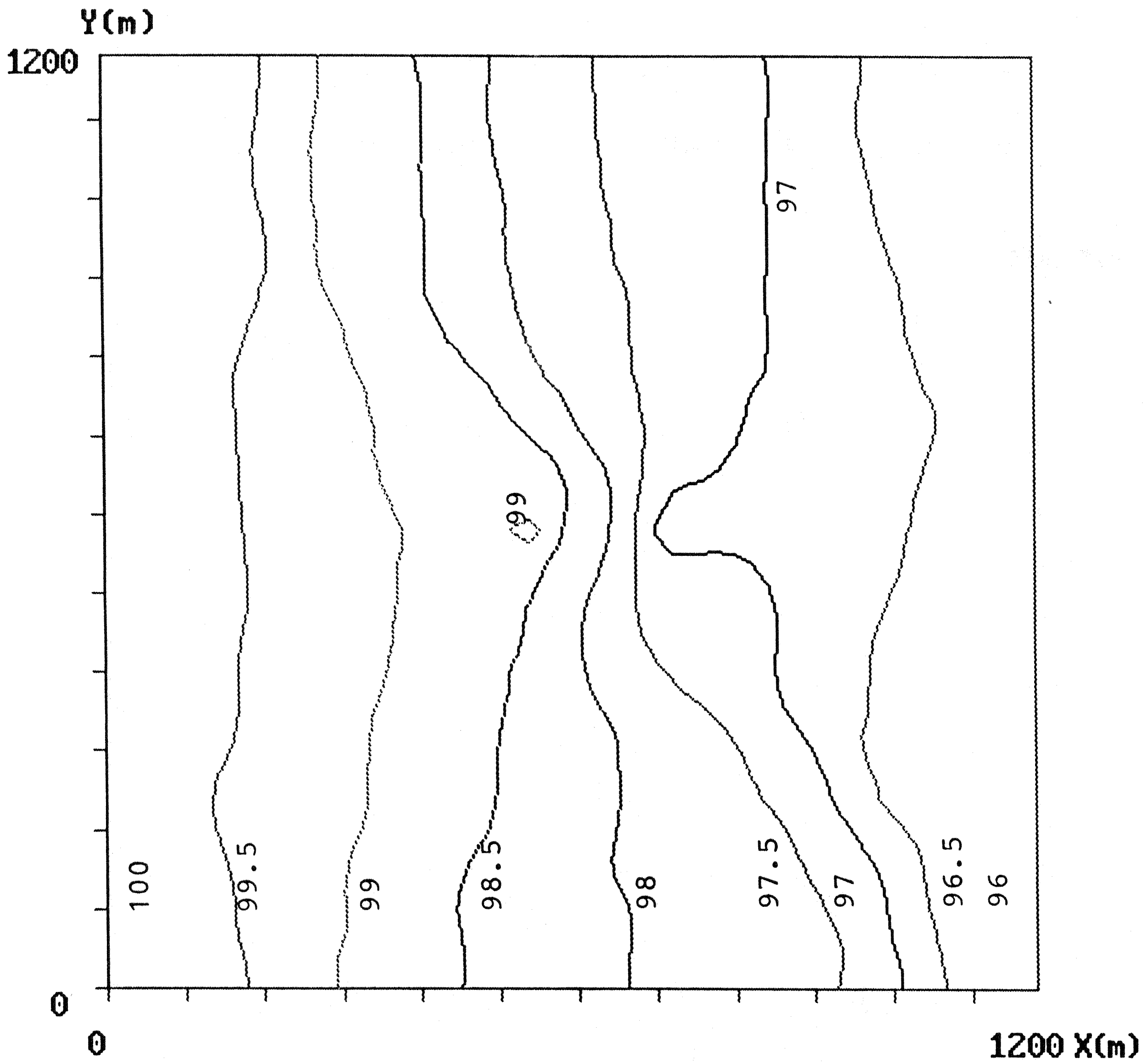

Figure 13 Head distribution calculated from field 2

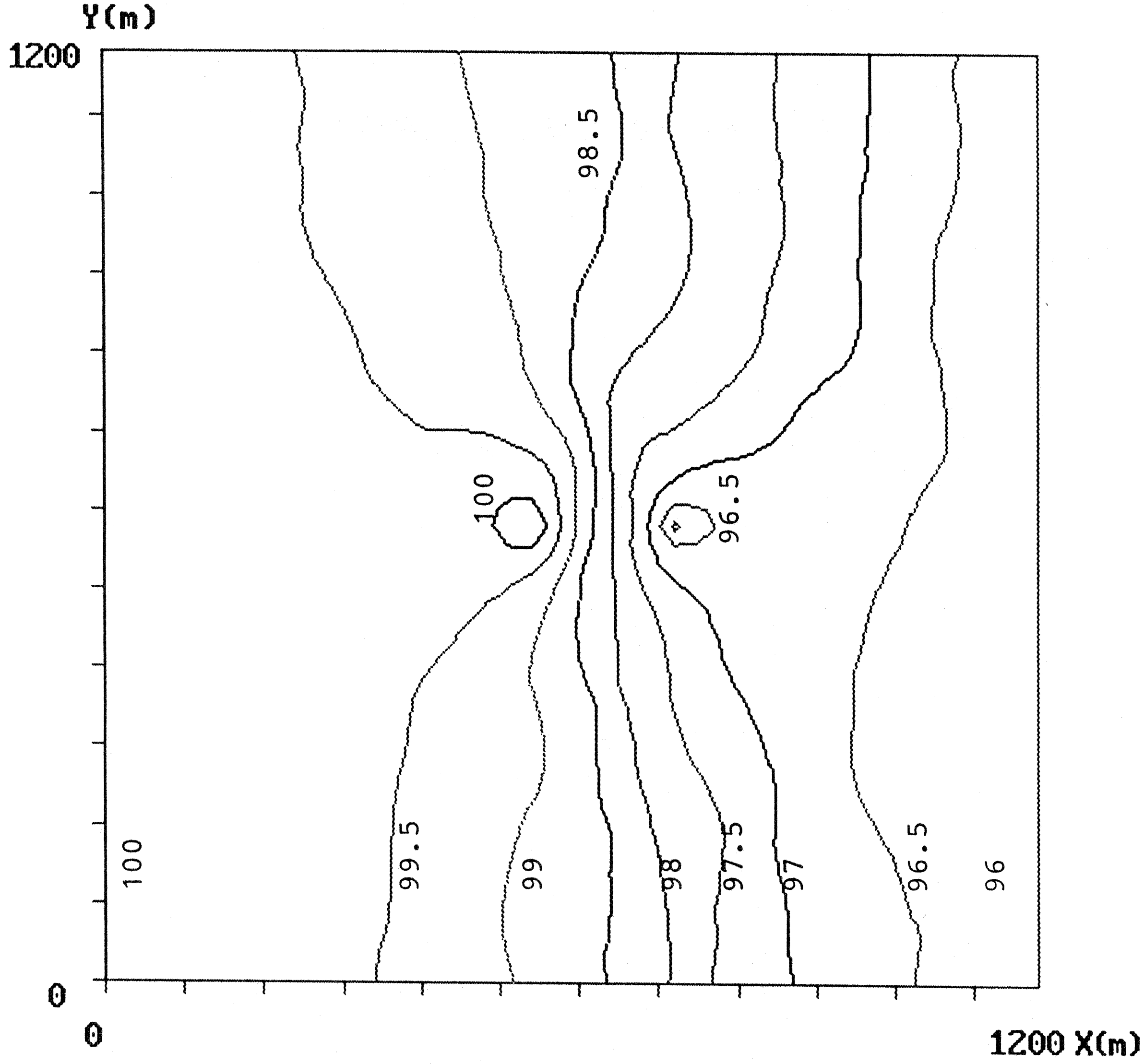

Figure 14 Head distribution calculated from field 3

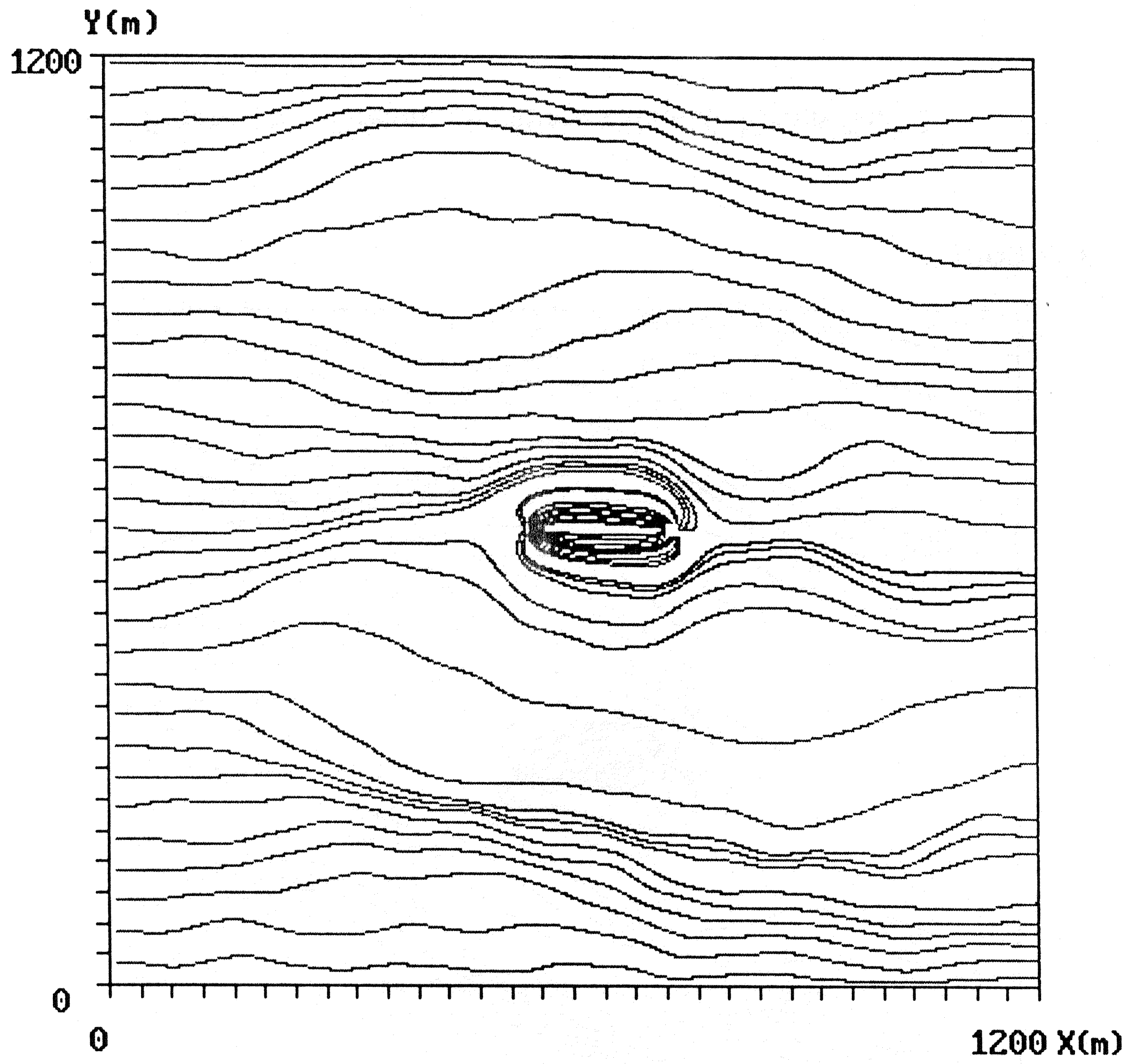

Figure 15   Streamline pattern calculated from field 1

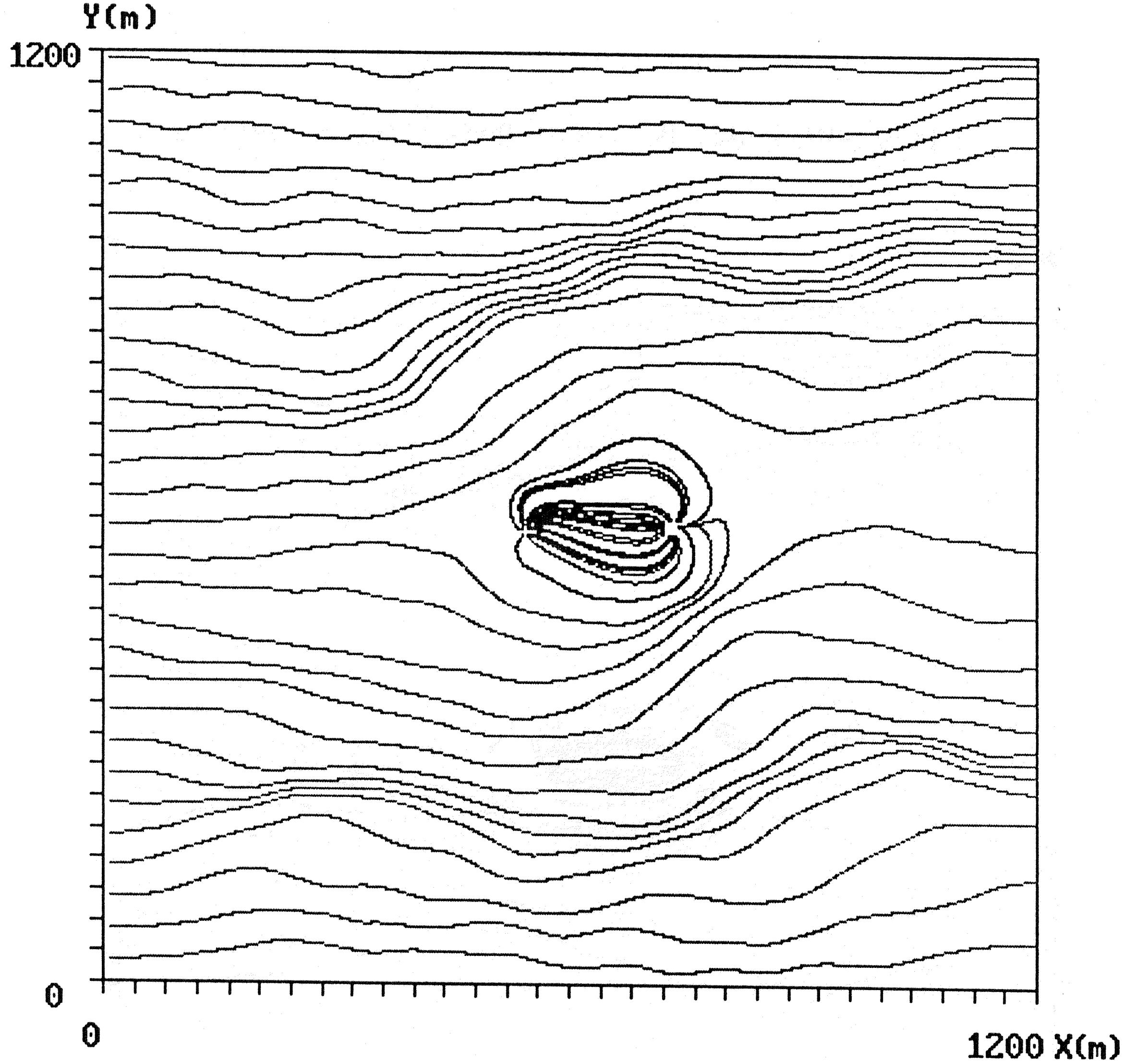

Figure 16 Streamline pattern calculated from field 2

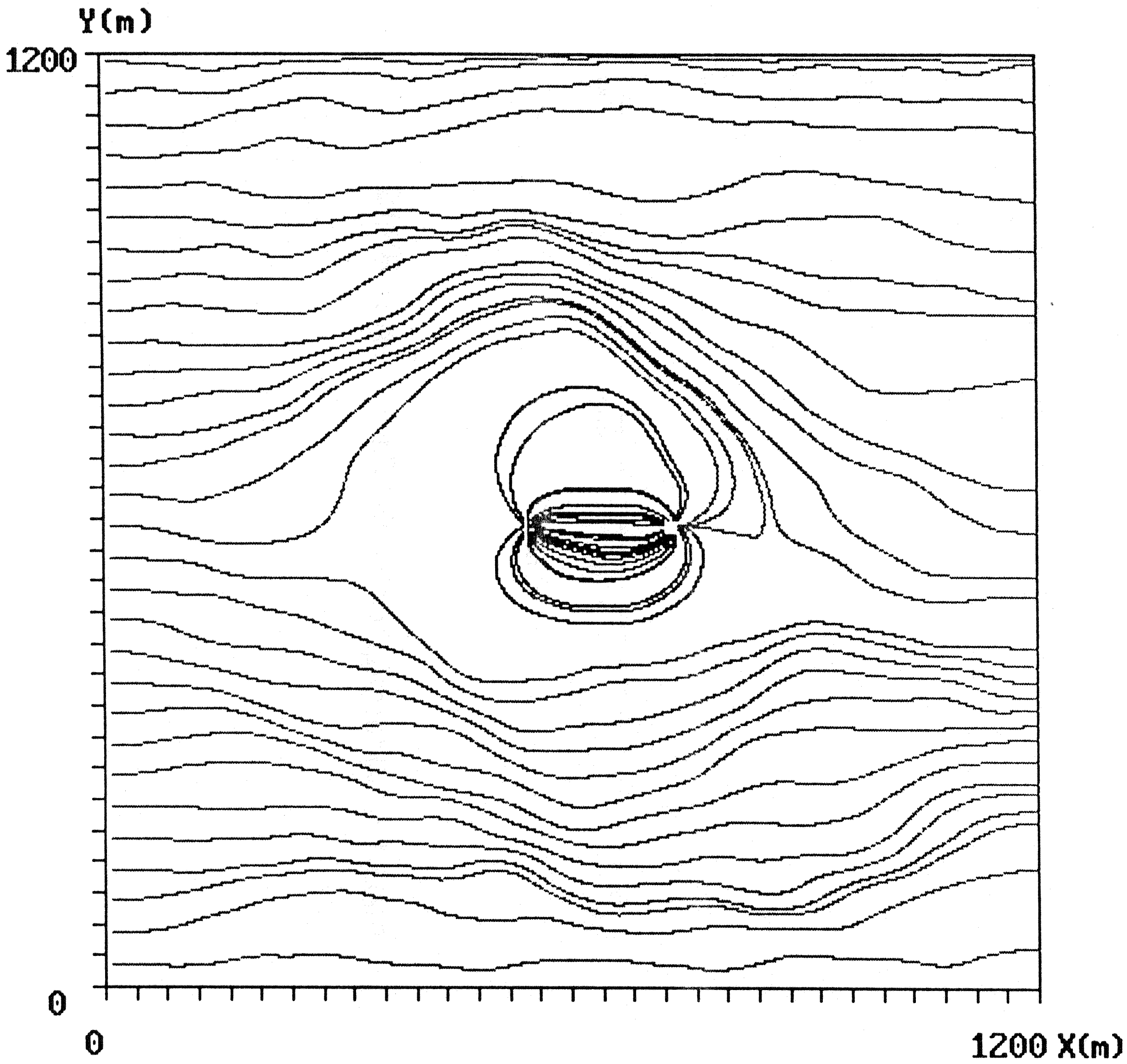

Figure 17   Streamline pattern calculated from field 3

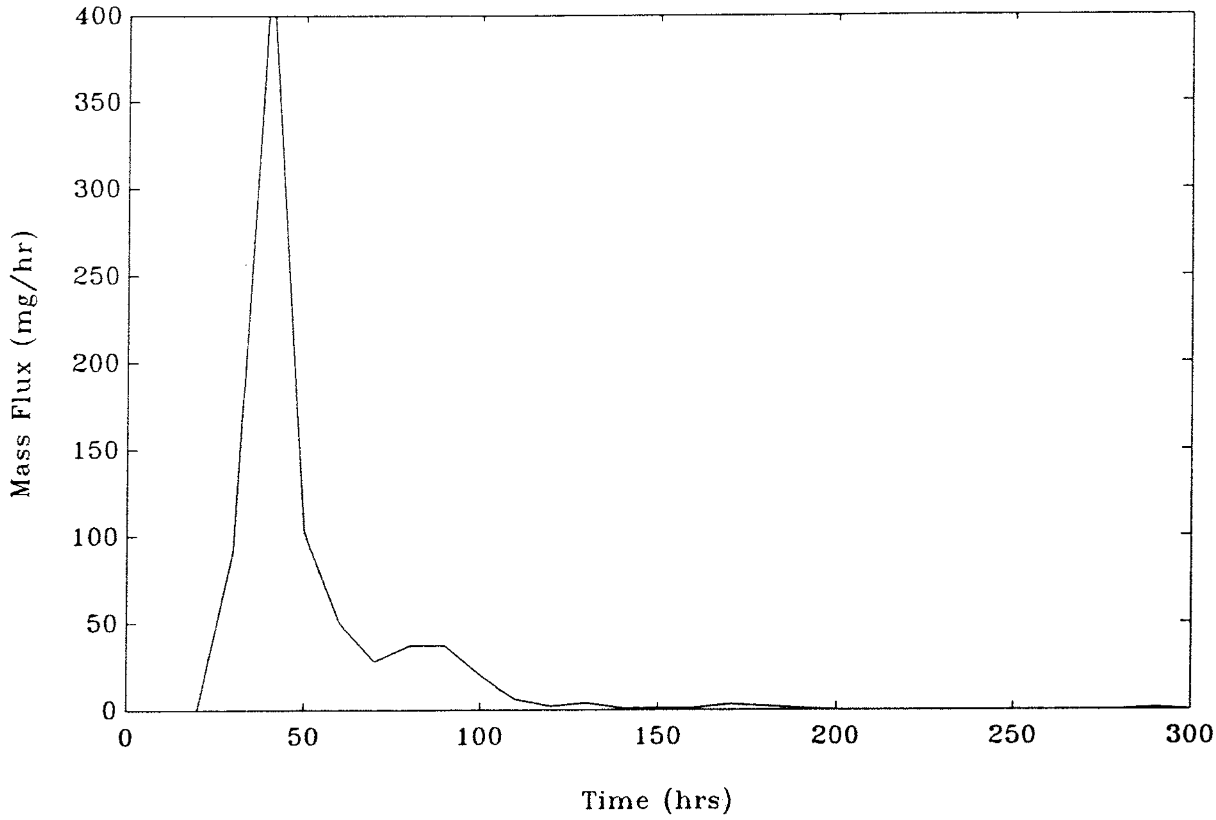

Figure 18 Field 1 breakthrough curve for Case 1 test at BFI02

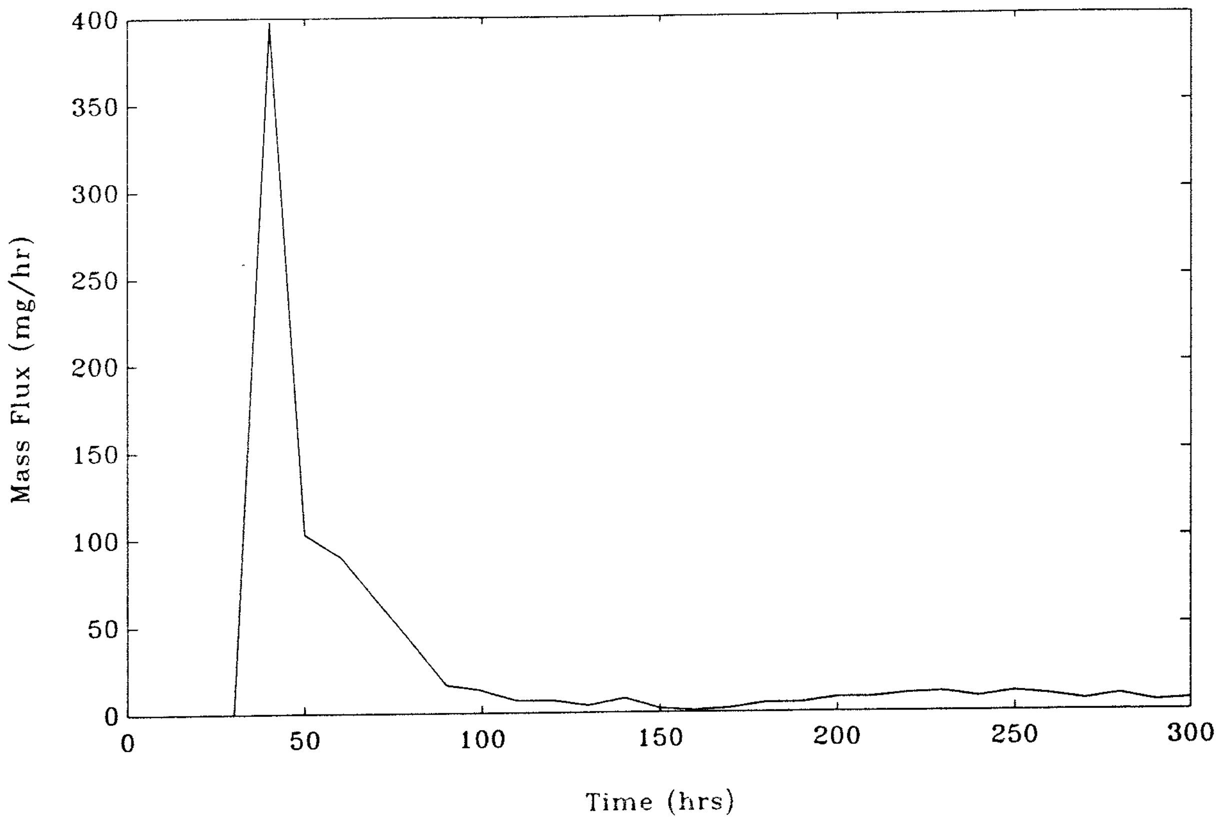

Figure 19 Field 2 breakthrough curve for Case 1 test at BFI02

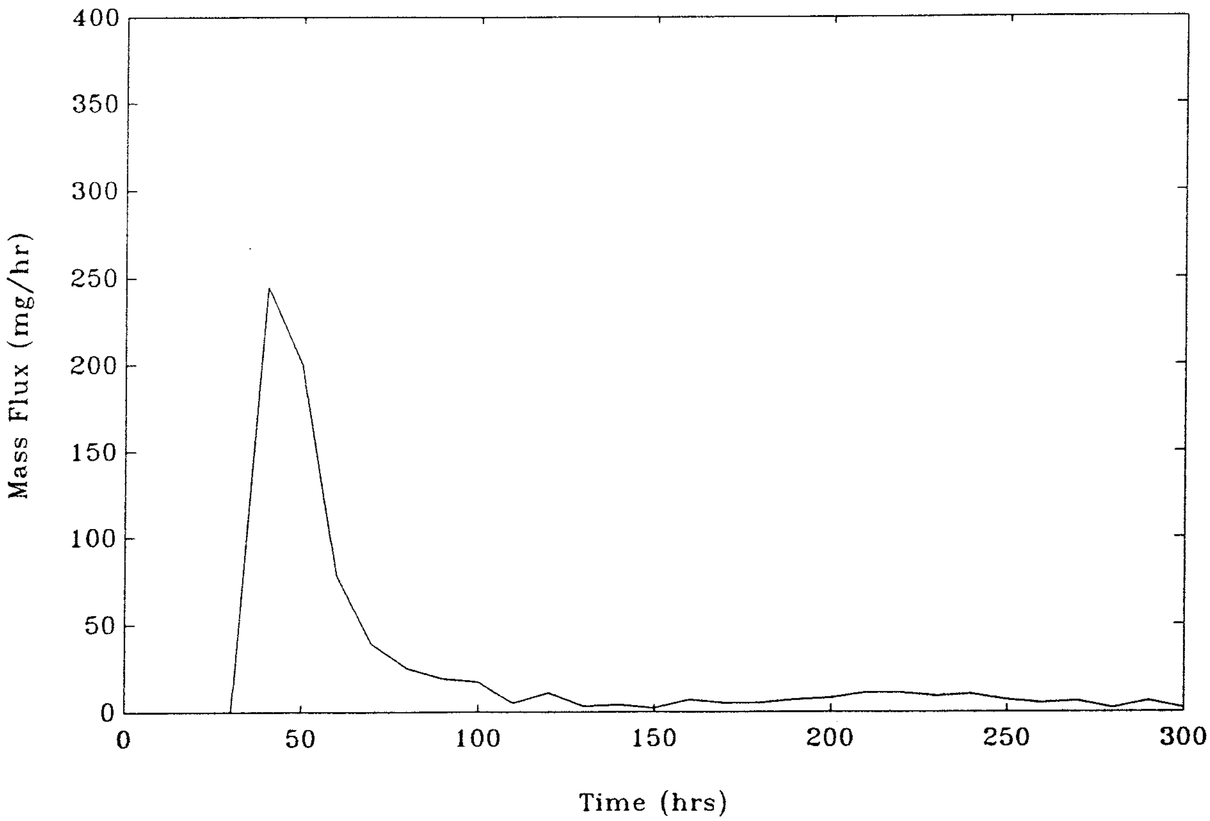

Figure 20 Field 3 breakthrough curve for Case 1 test at BFI02

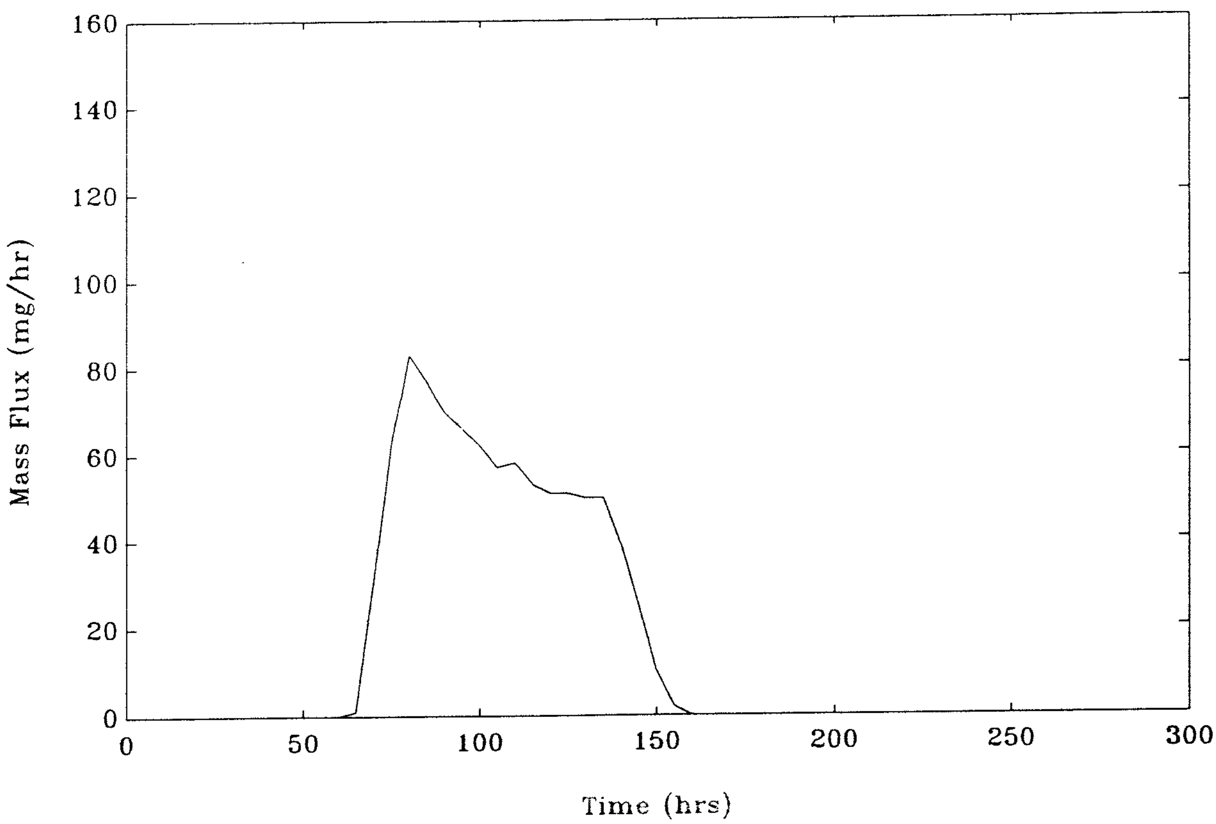

Figure 21 Field 2 breakthrough curve for Case 2 test at BFI02

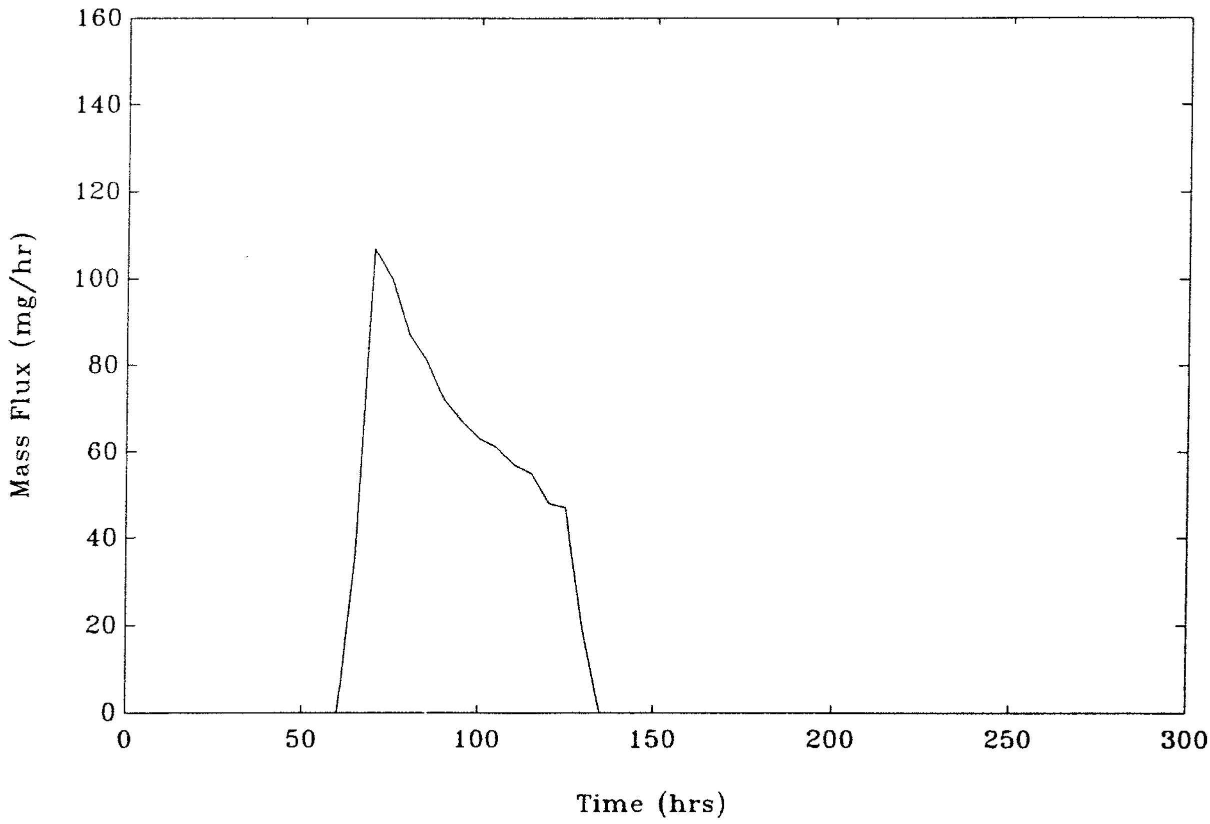

Figure 22 Field 3 breakthrough curve for Case 2 test at BFI02

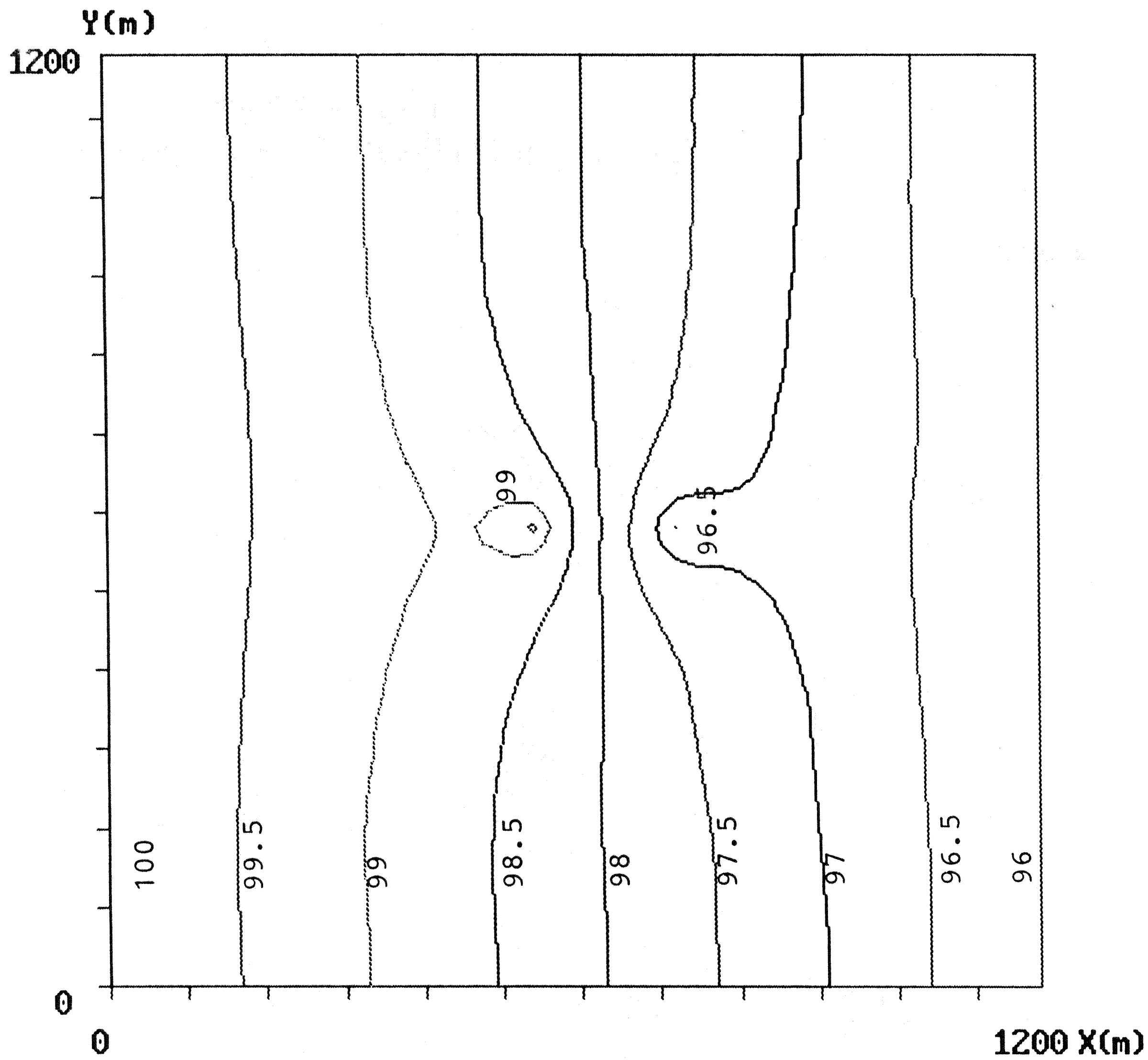

Figure 23 Ensemble mean head distribution of conditional simulation fields

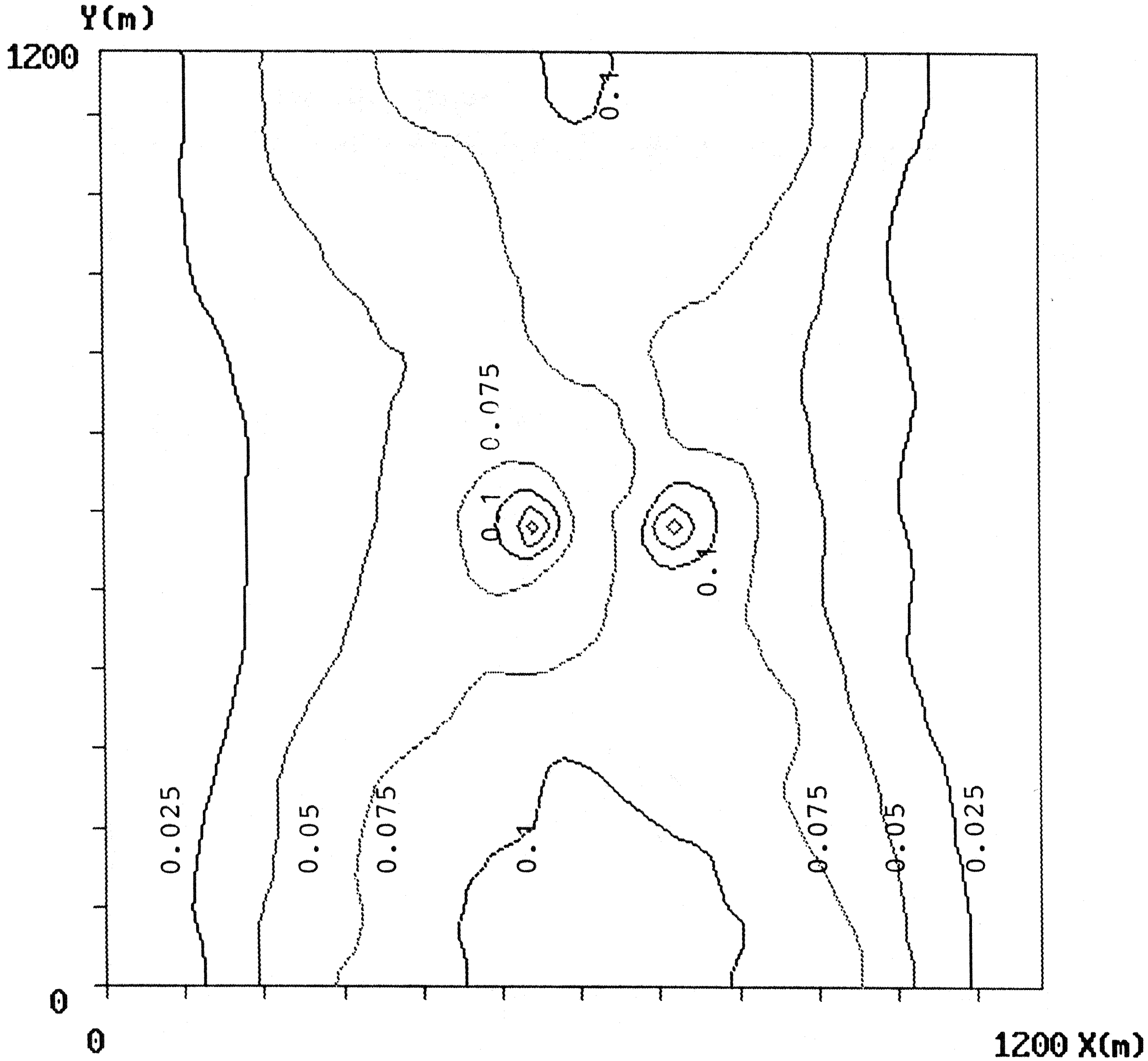

Figure 24 Variance of head distribution of conditional simulation fields

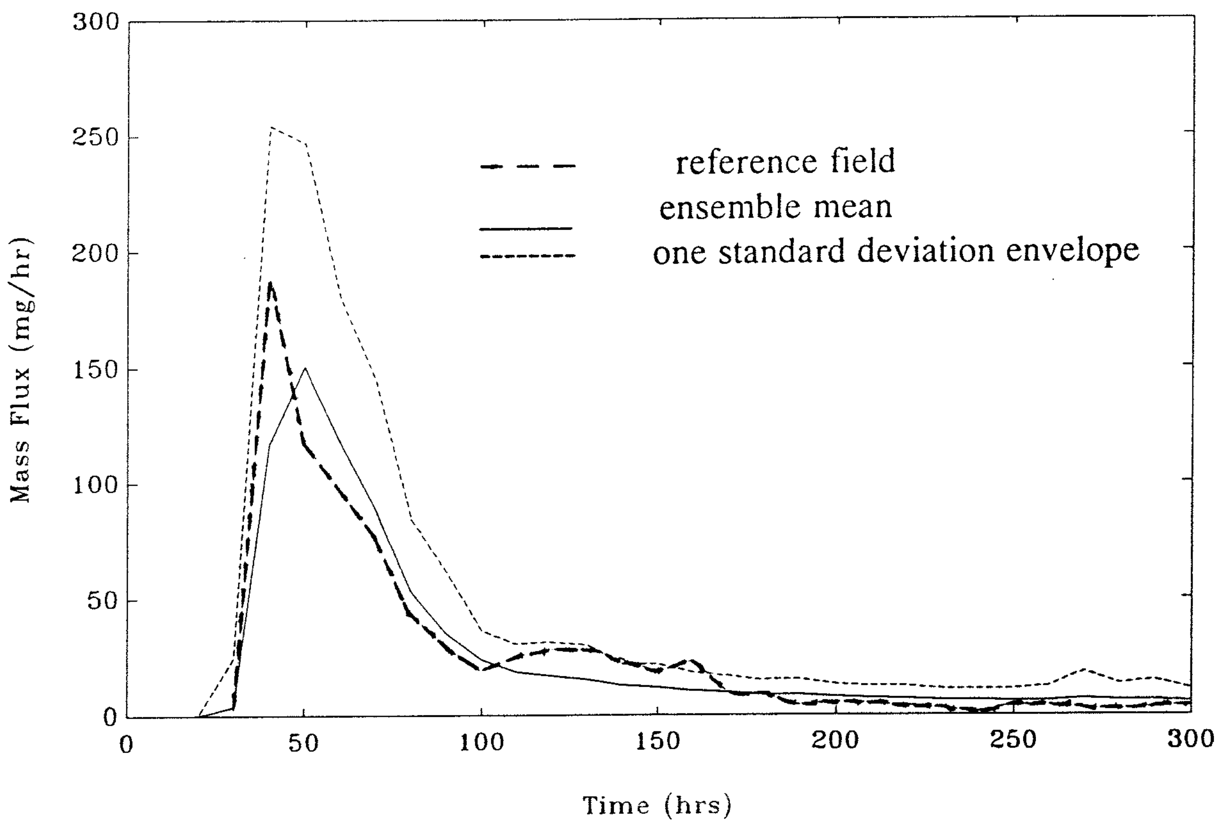

Figure 25 Ensemble mean breakthrough curve for Case 1 test at BFI02

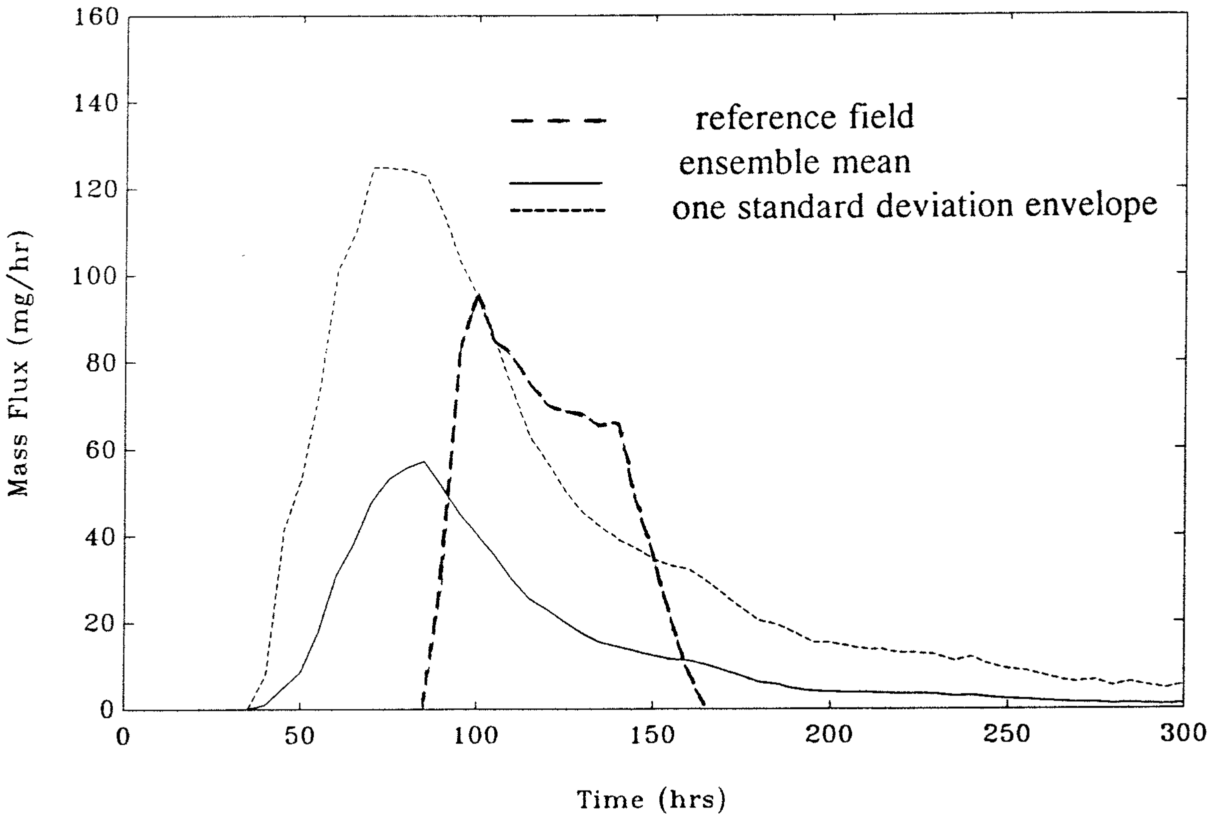

Figure 26   Ensemble mean breakthrough curve for Case 2 test at BFI02

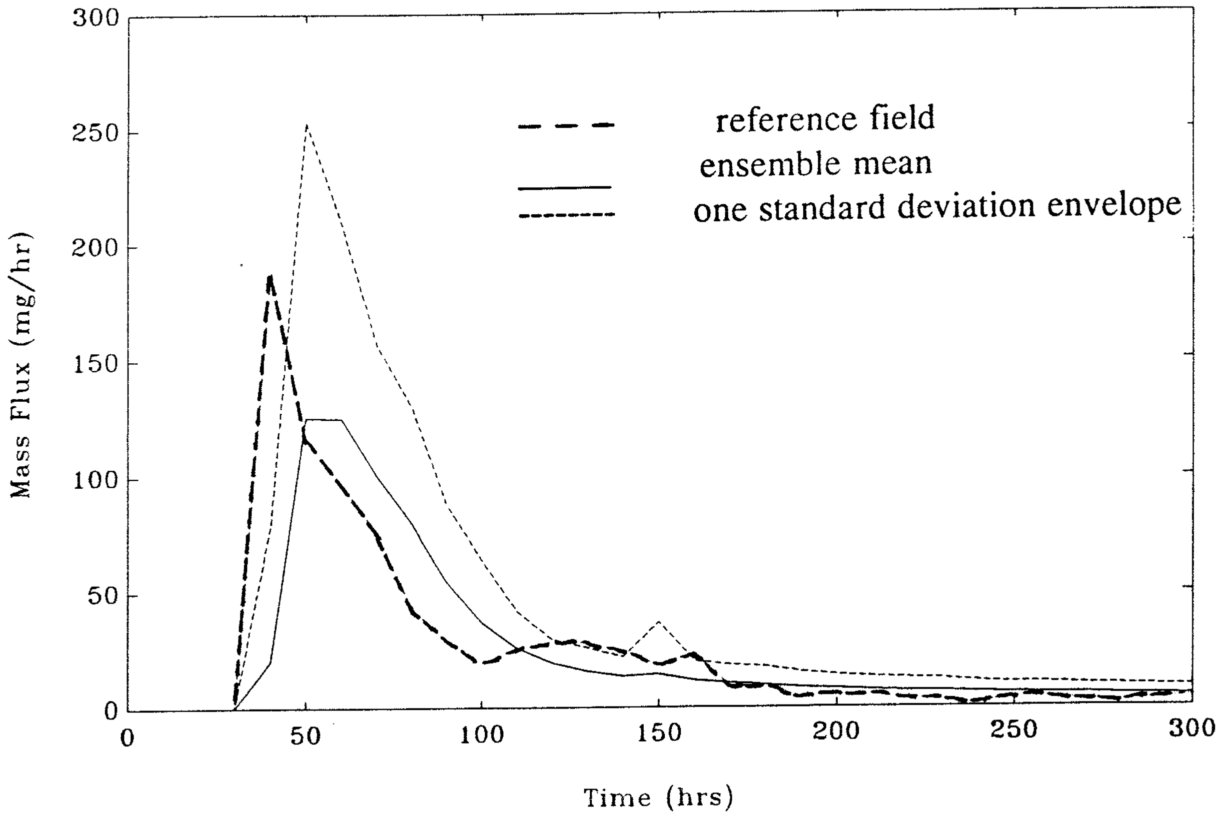

Figure 27 Ensemble mean breakthrough curve for Case 1 test at BFI02 (porosity, n=0.03)

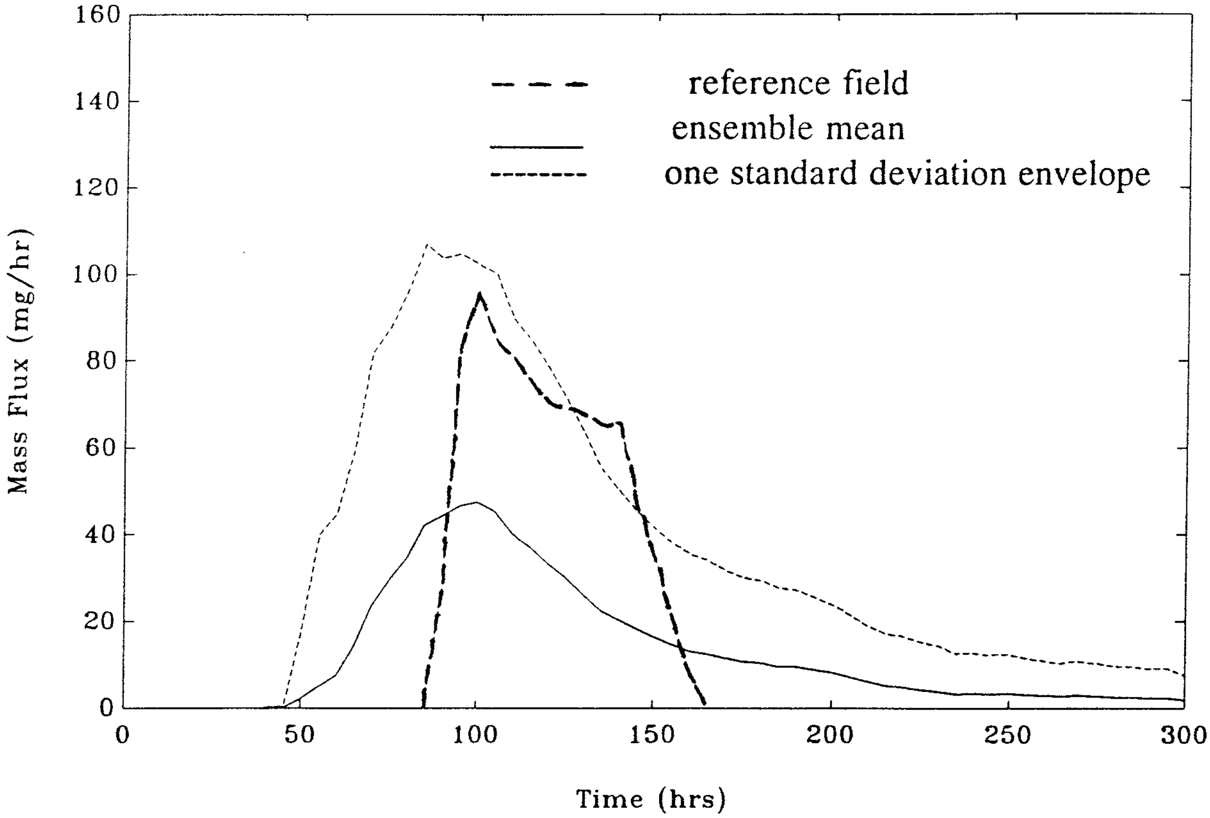

Figure 28 Ensemble mean breakthrough curve for Case 2 test at BFI02 (porosity, n=0.03)

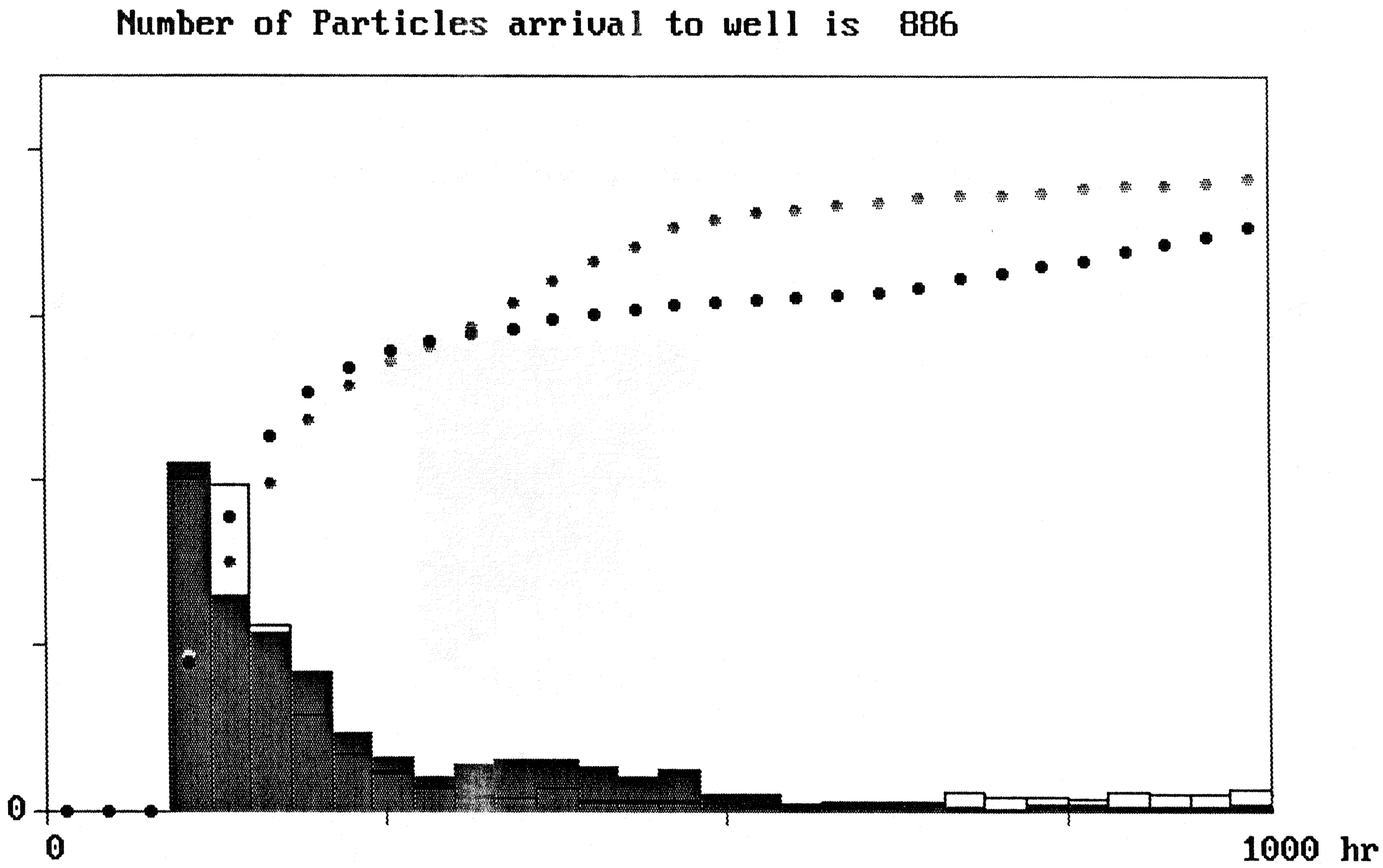

Figure 29 Breakthrough curve for Case 1 test of field 22.
Dark bars and grey dots = reference field
Unfilled bars and black dots = field #

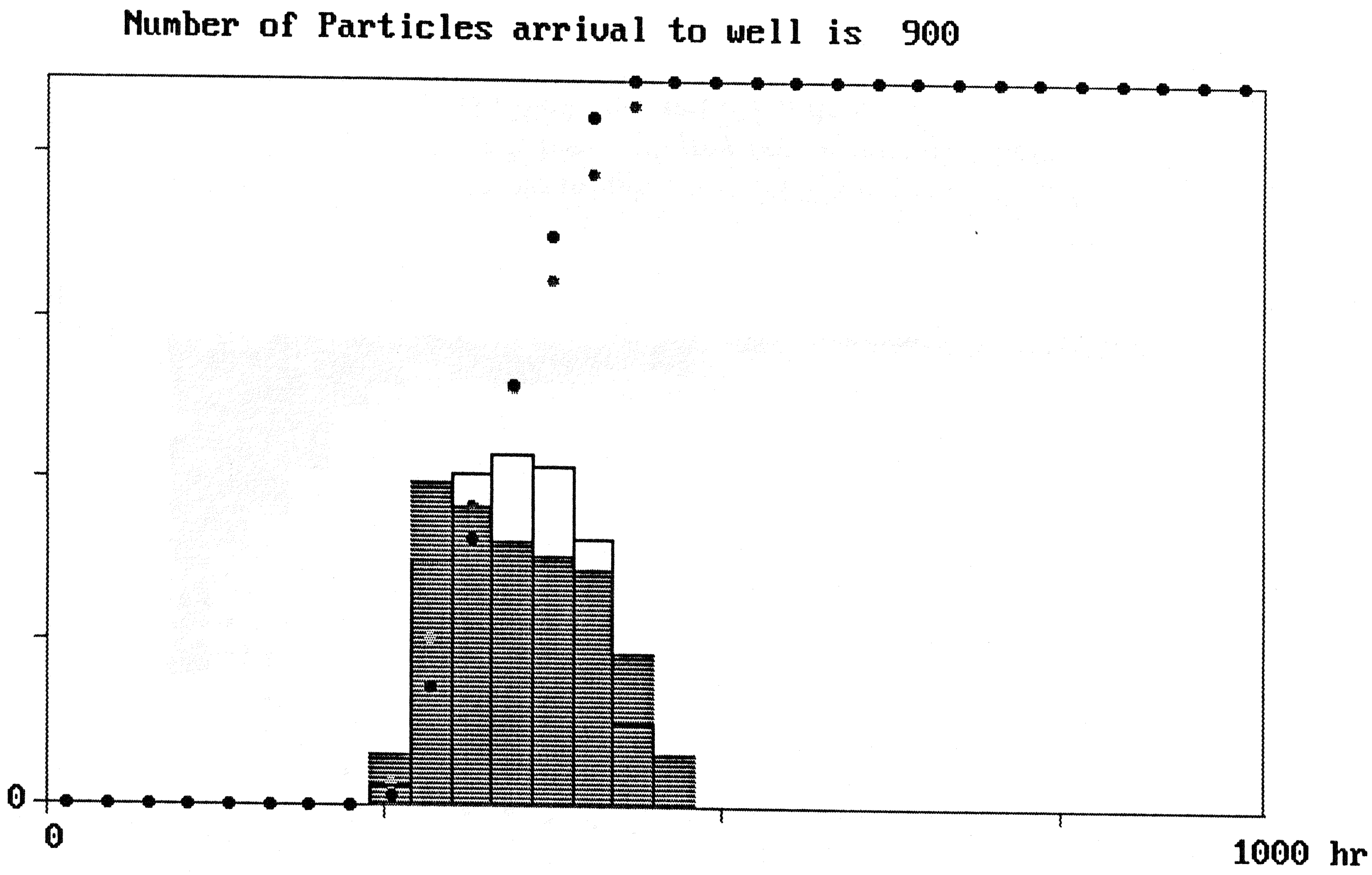

Figure 30 Breakthrough curve for Case 2 test of field 22

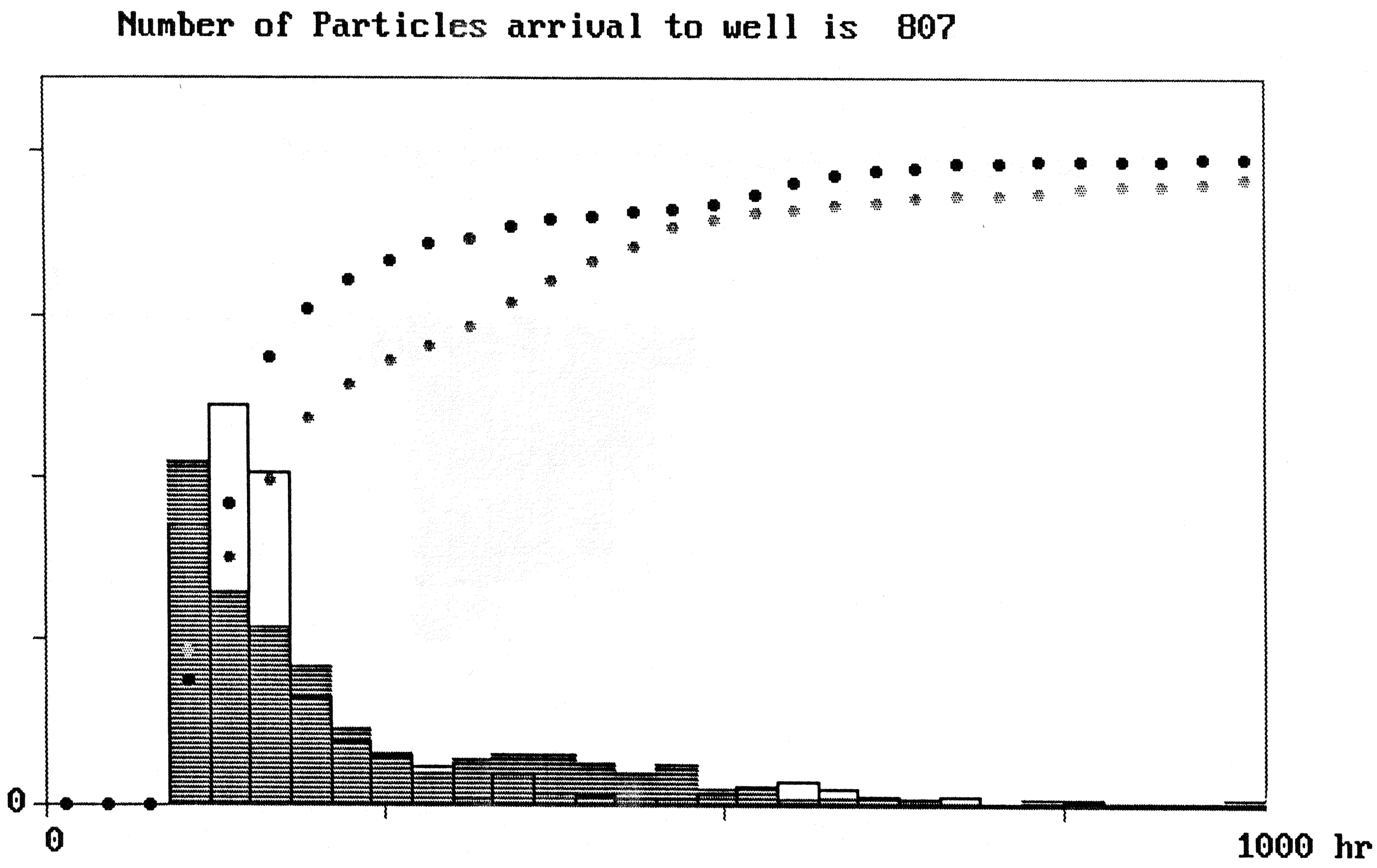

Figure 31 Breakthrough curve for Case 1 test of field 38

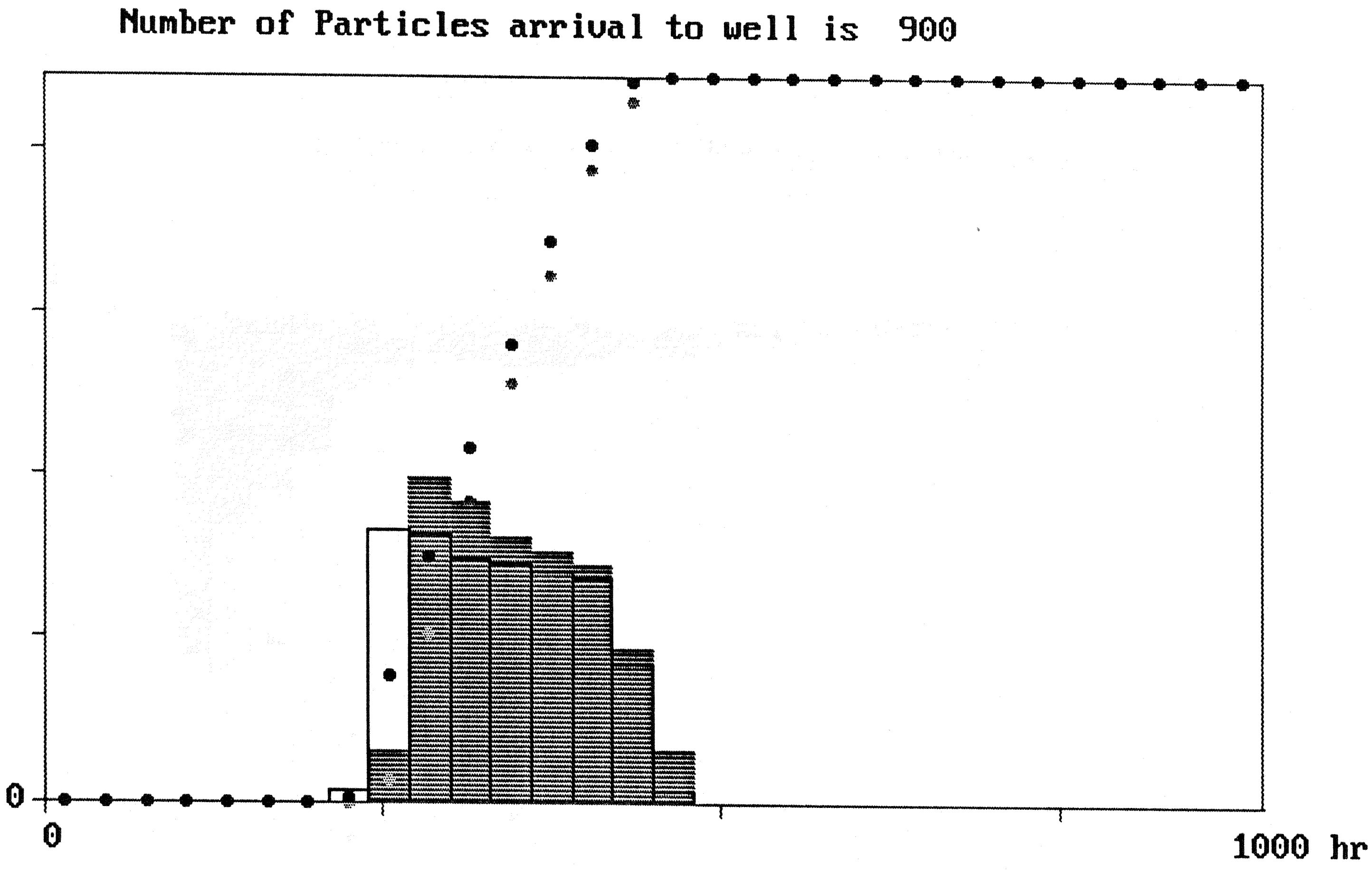

Figure 32 Breakthrough curve for Case 2 test of field 38

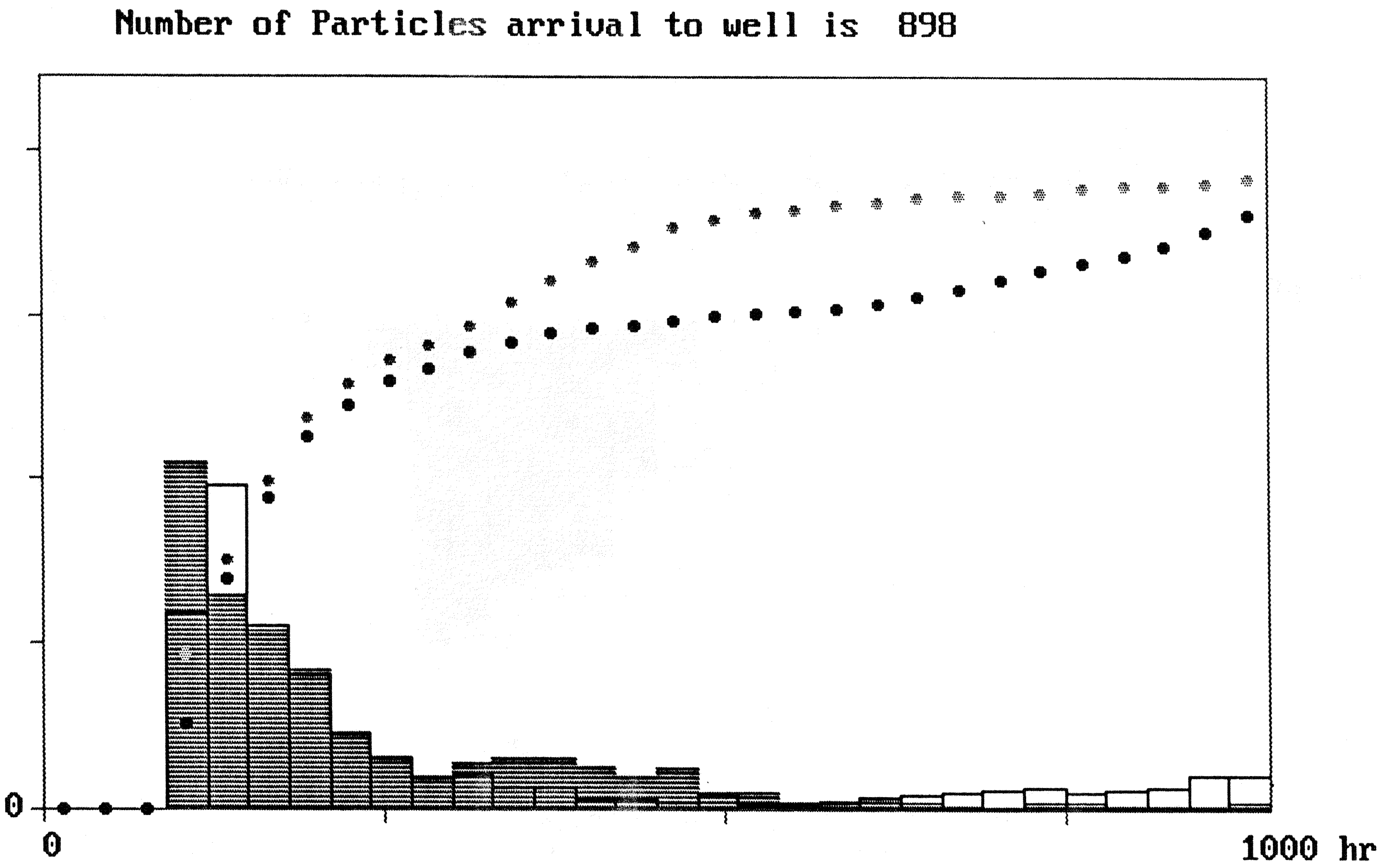

Figure 33 Breakthrough curve for Case 1 test of field 96

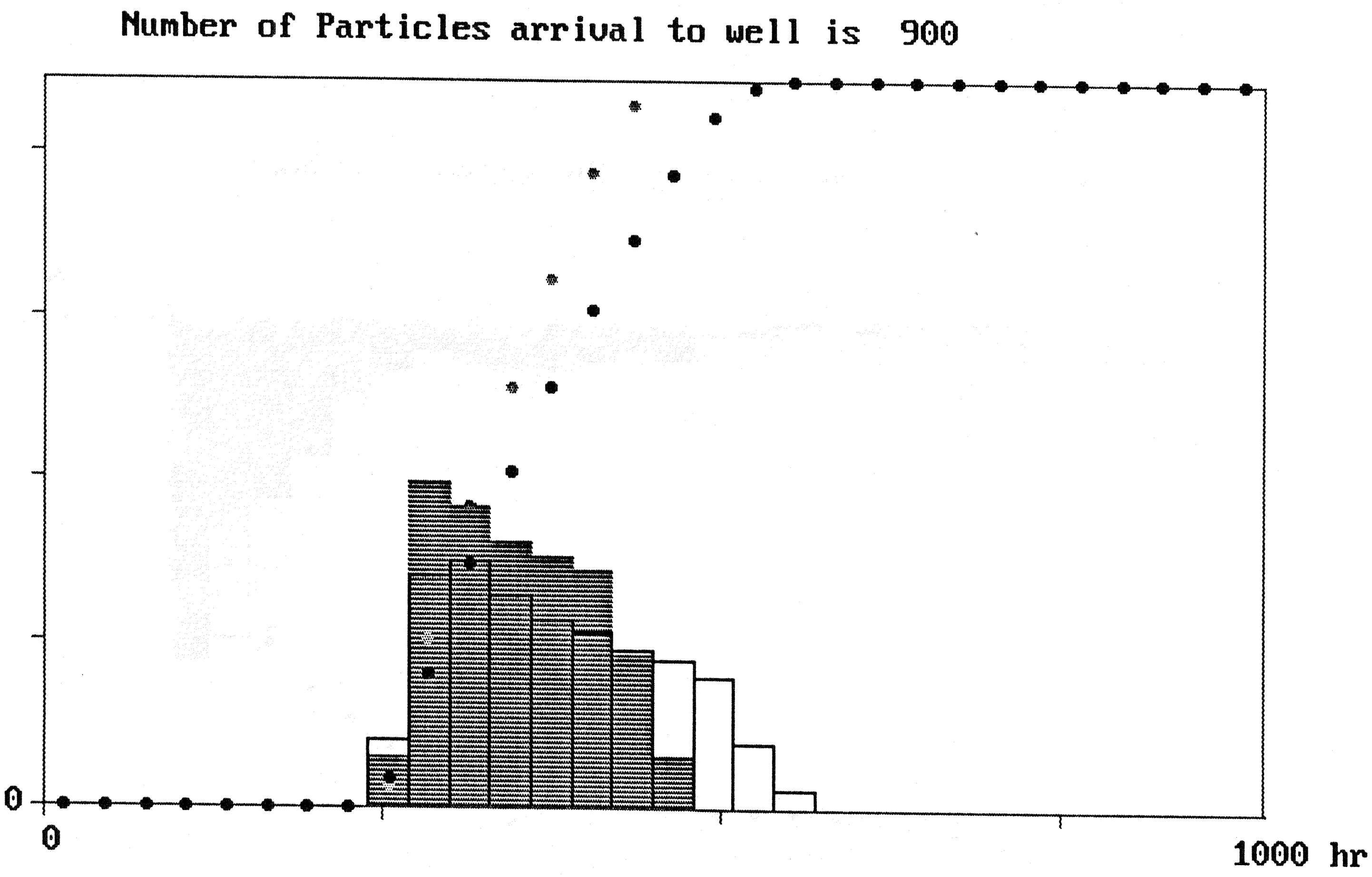

Figure 34 Breakthrough curve for Case 2 test of field 96

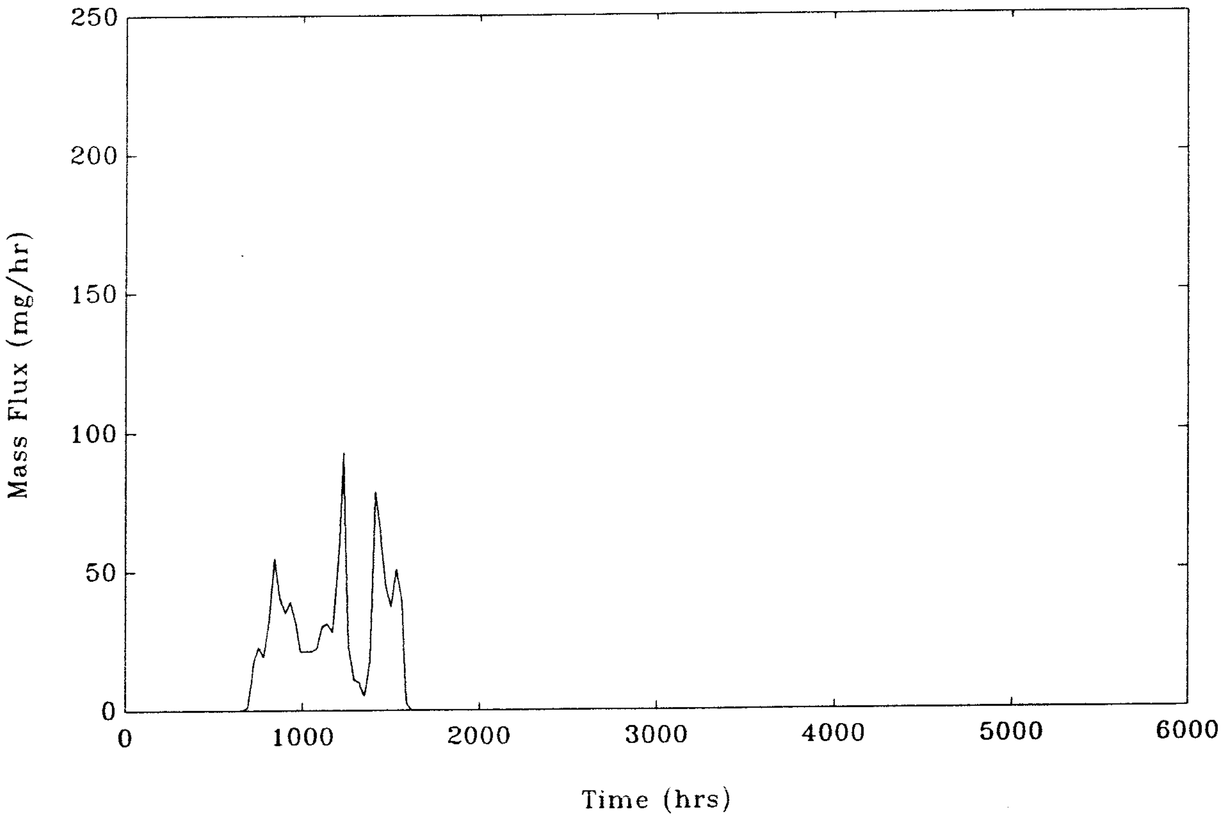

Figure 35 Field 1 breakthrough curve for far field simulation

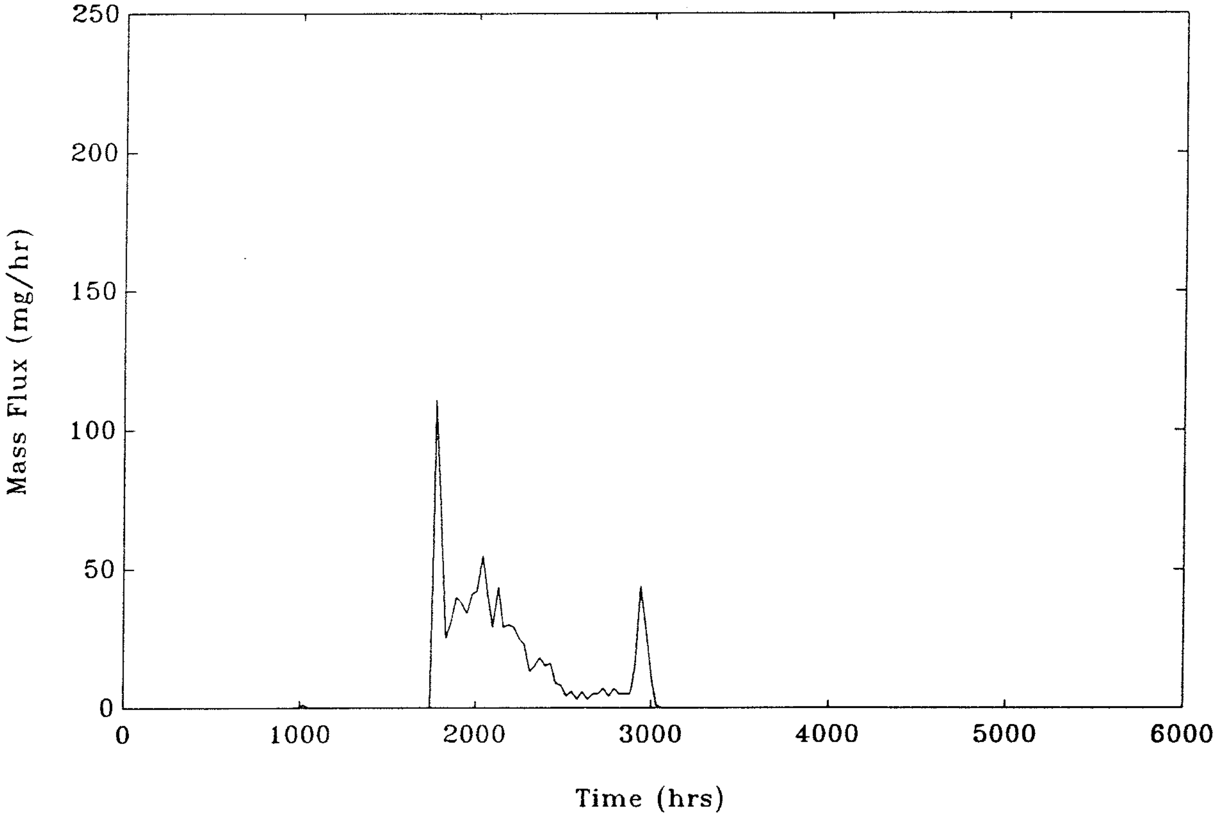

Figure 36 Field 2 breakthrough curve for far field simulation

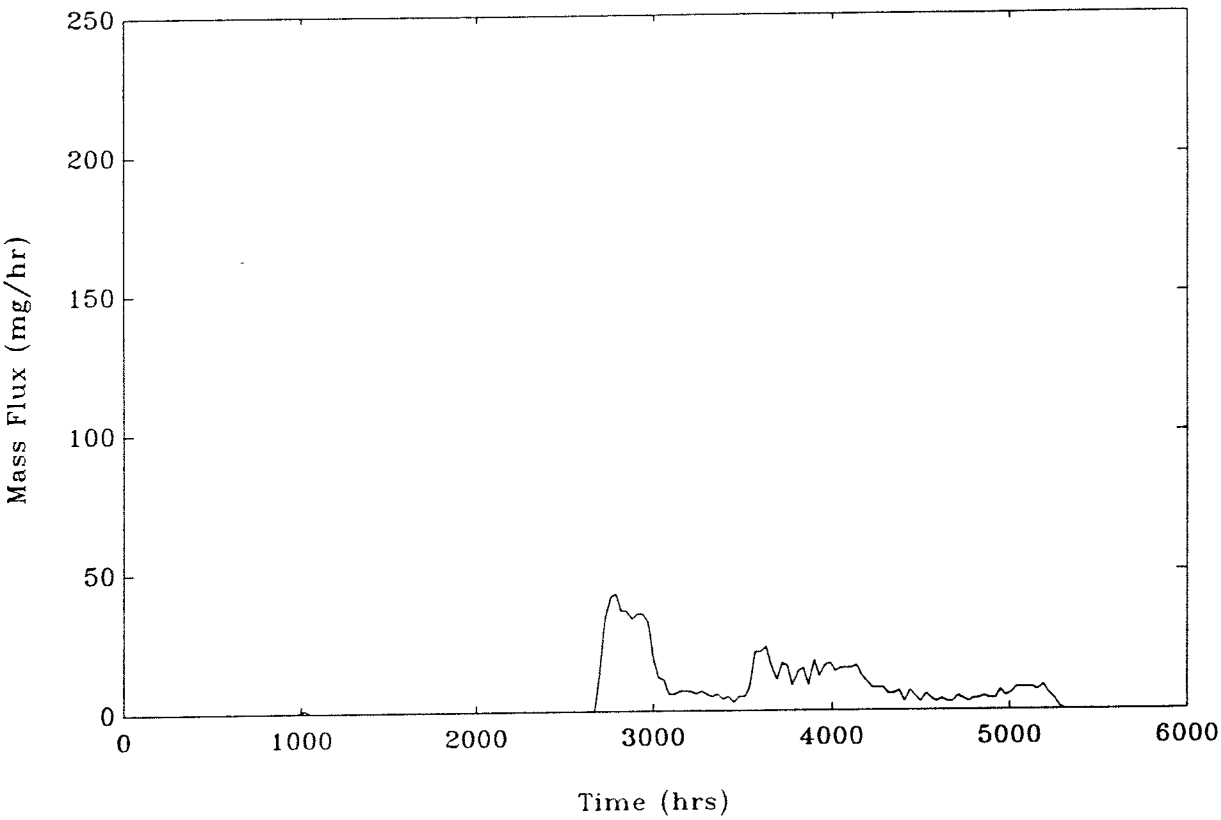

Figure 37 Field 3 breakthrough curve for far field simulation

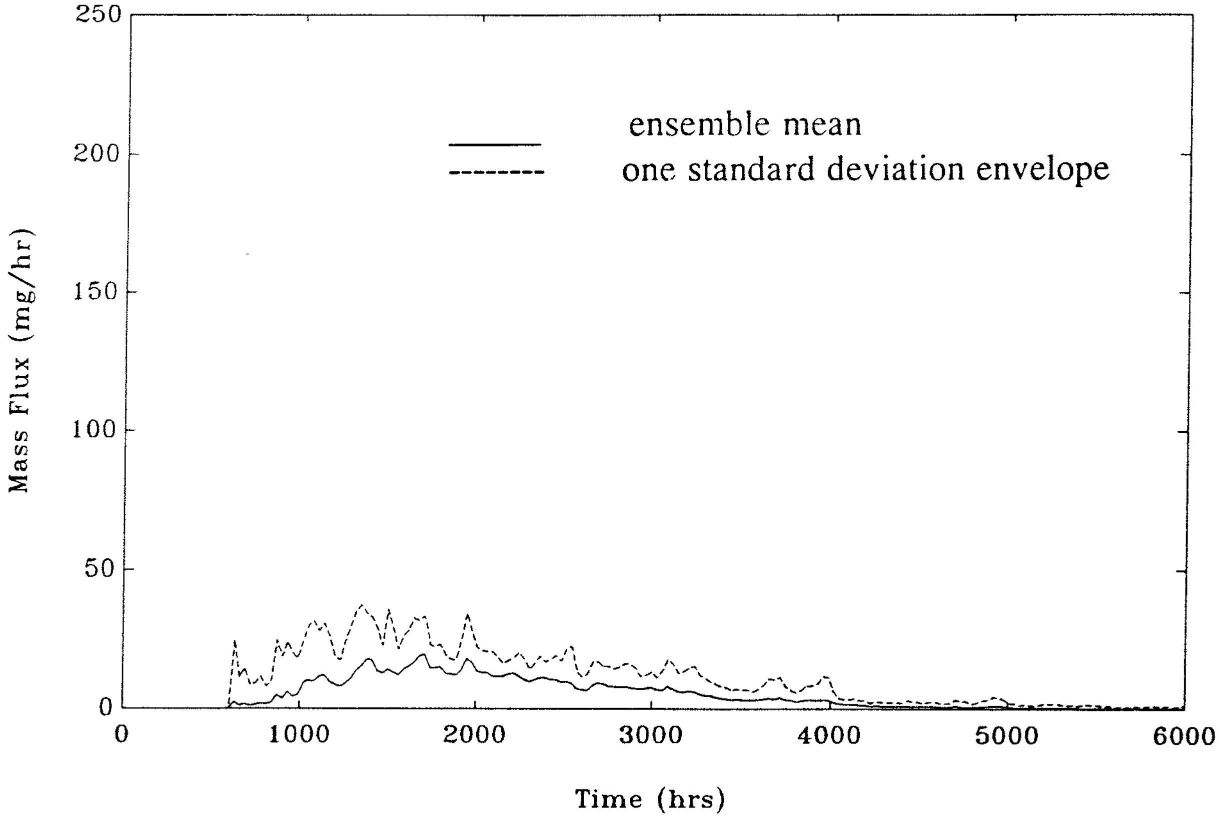

Figure 38 Ensemble mean breakthrough curve for far field simulation (8 points conditioning)

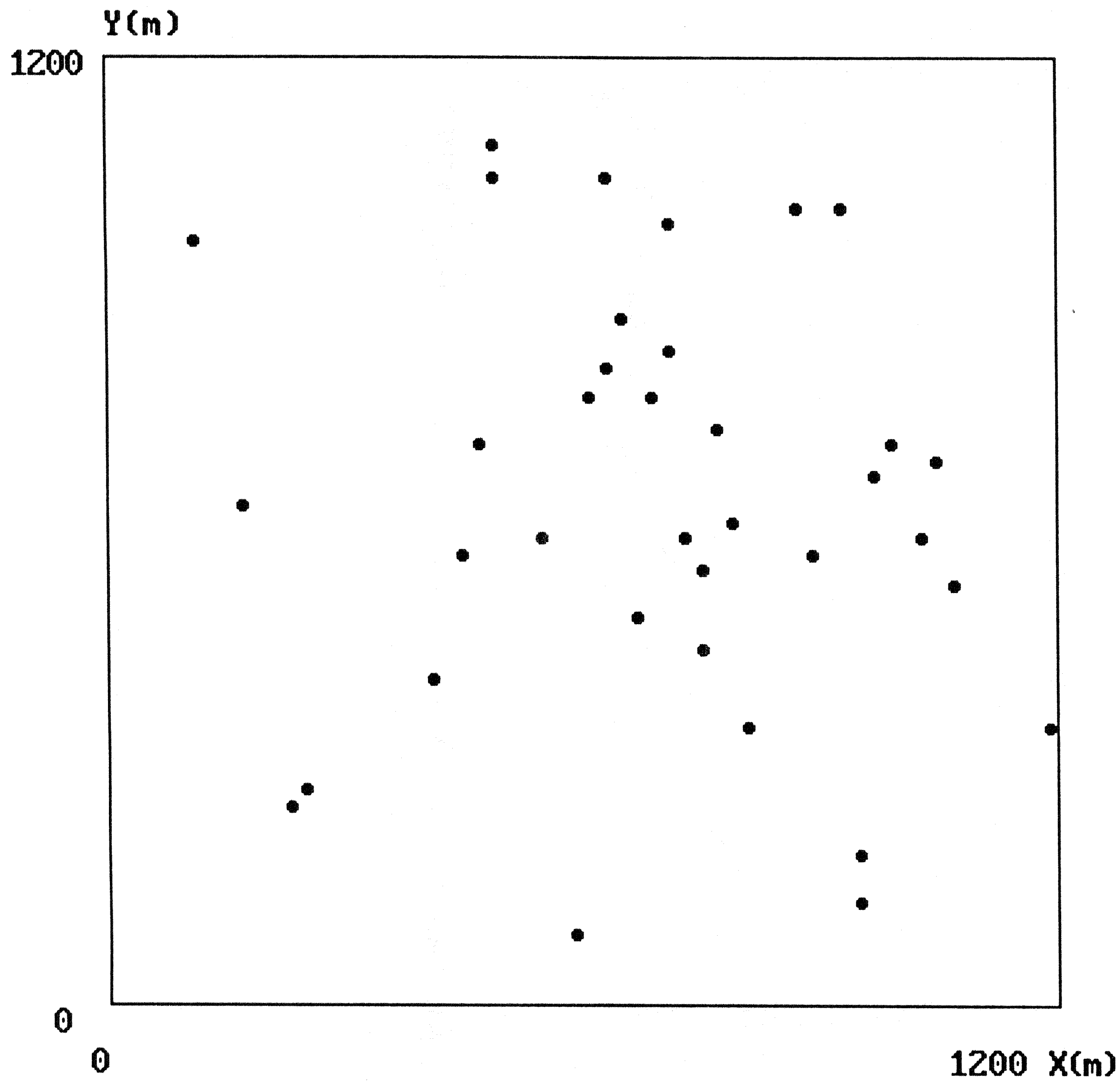

Figure 39   New measurement locations in the reference field

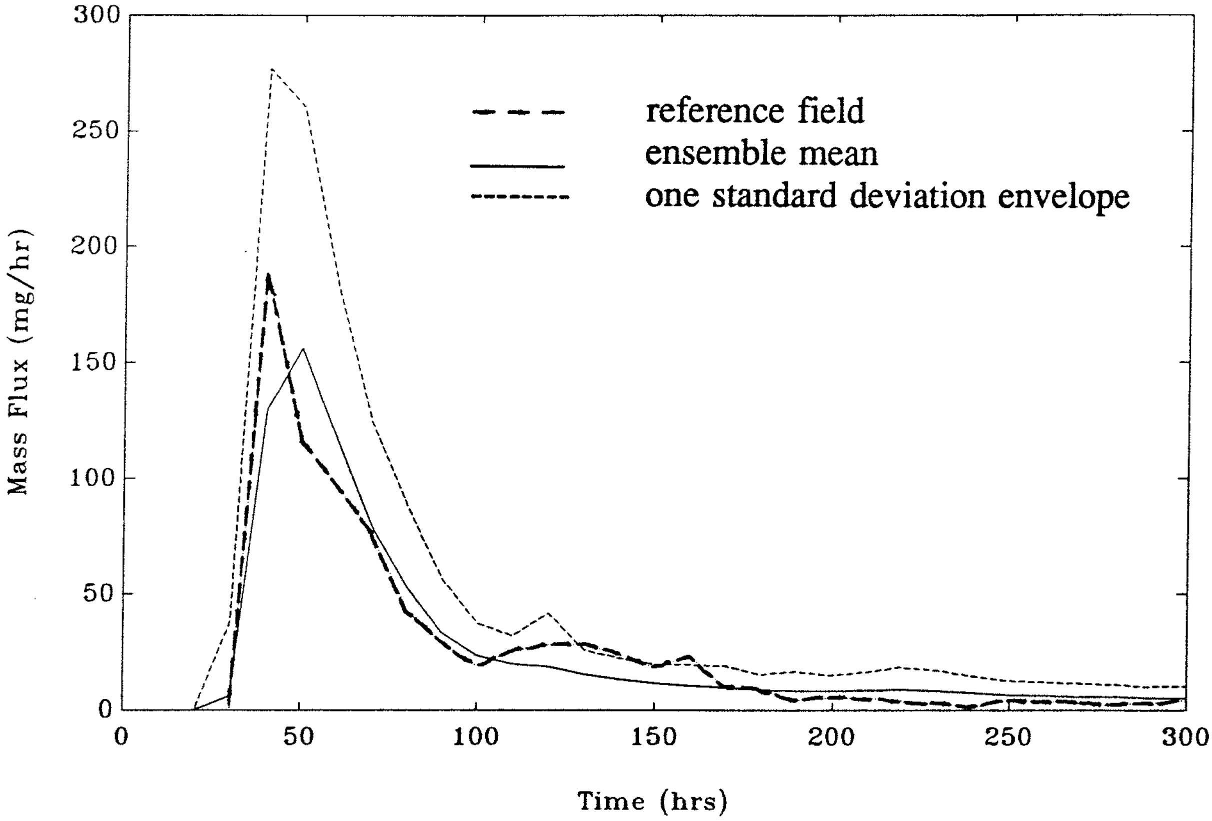

Figure 40 Ensemble mean breakthrough curve for case 1 test at BFI02
(36 points conditioning)

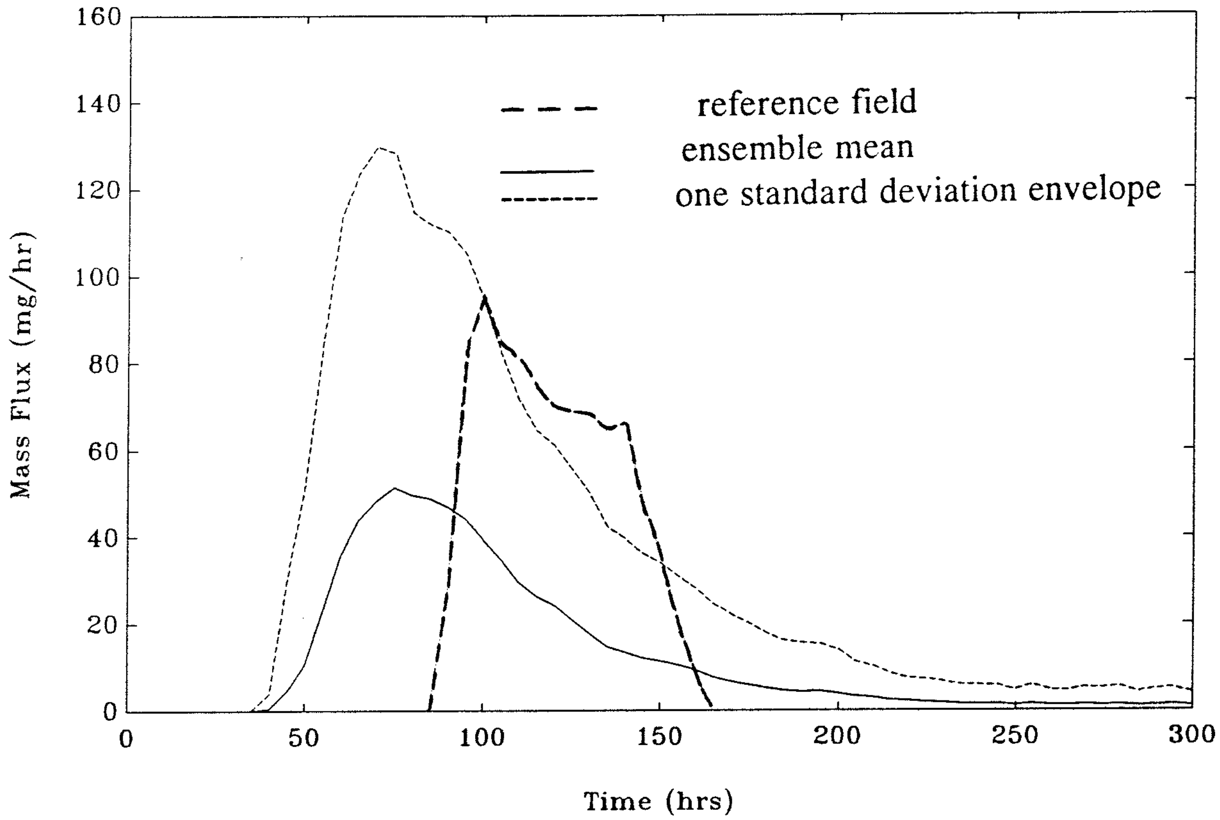

Figure 41 Ensemble mean breakthrough curve for Case 2 test at BFI02 (36 point conditioning)

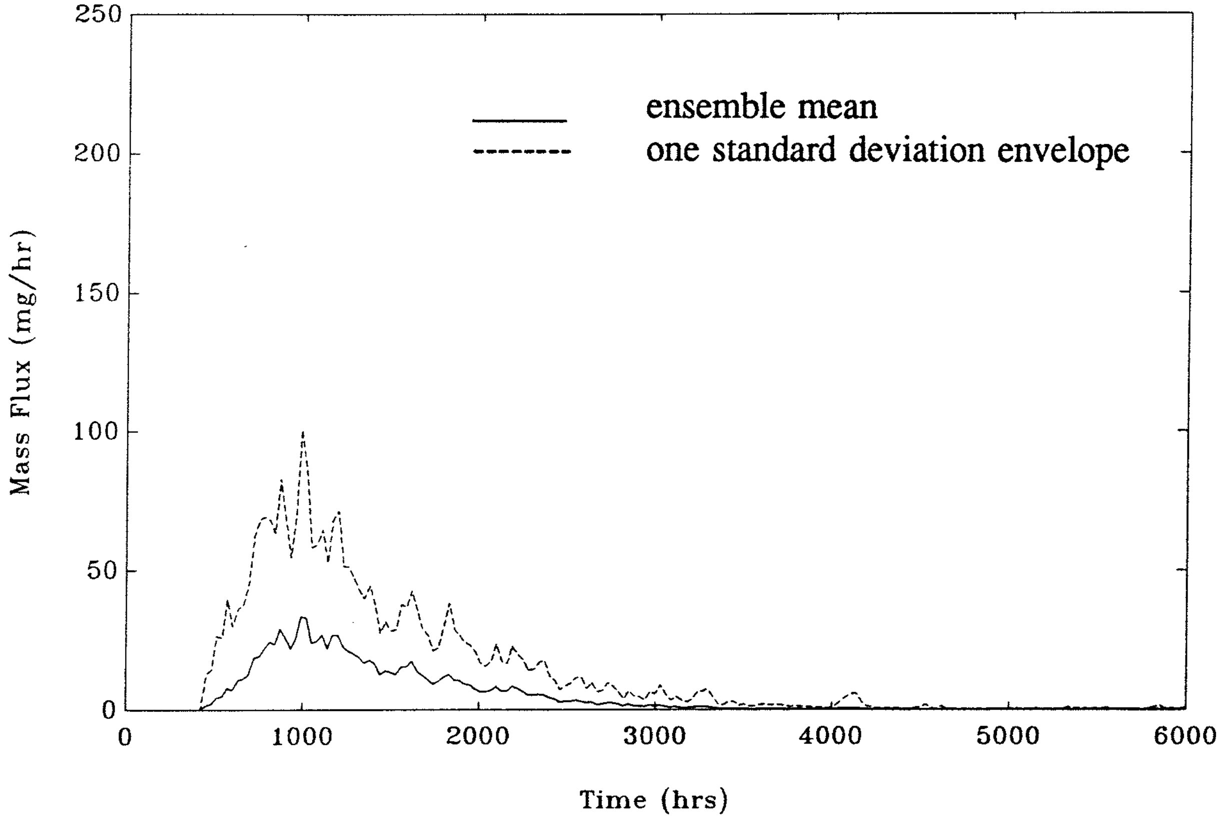

Figure 42 Ensemble mean breakthrough curve of far field simulation (36 point conditioning)

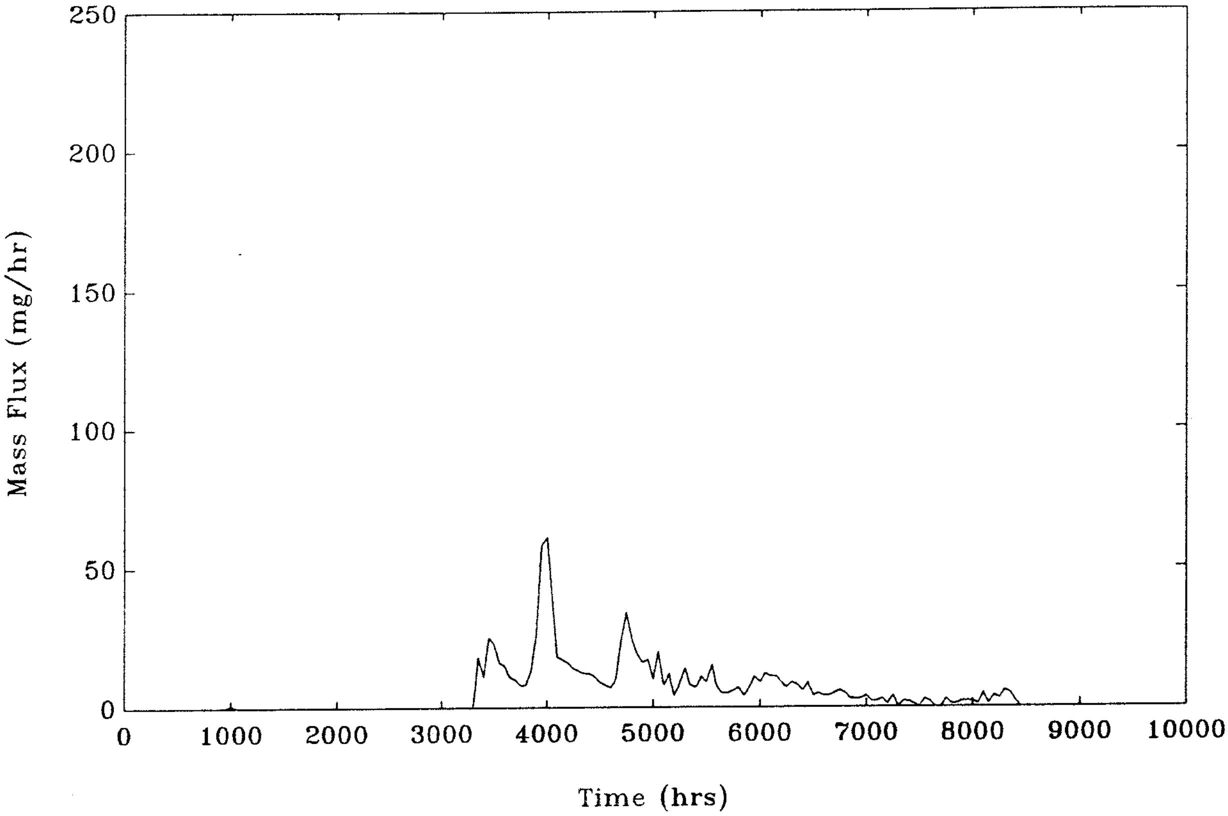

Figure 43   Field 22 breakthrough curve for far field simulation

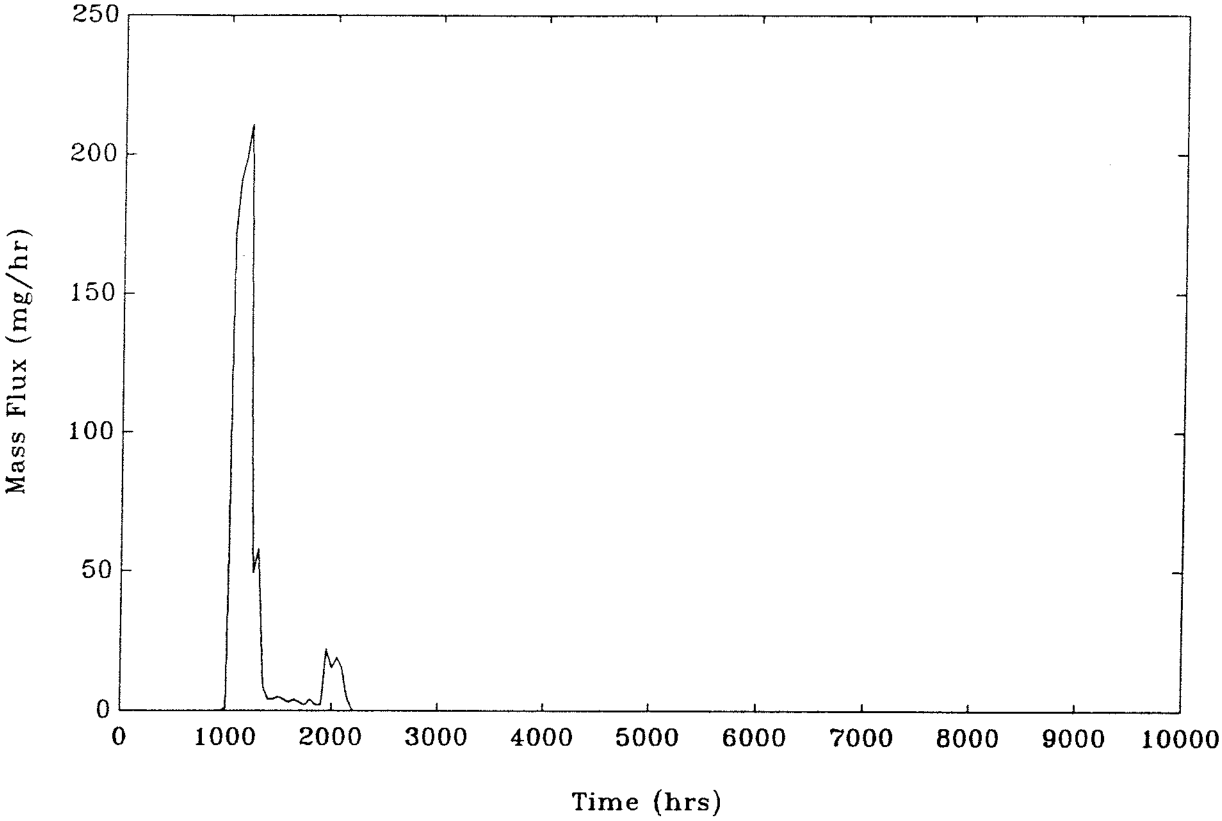

Figure 44   Field 38 breakthrough curve for far field simulation

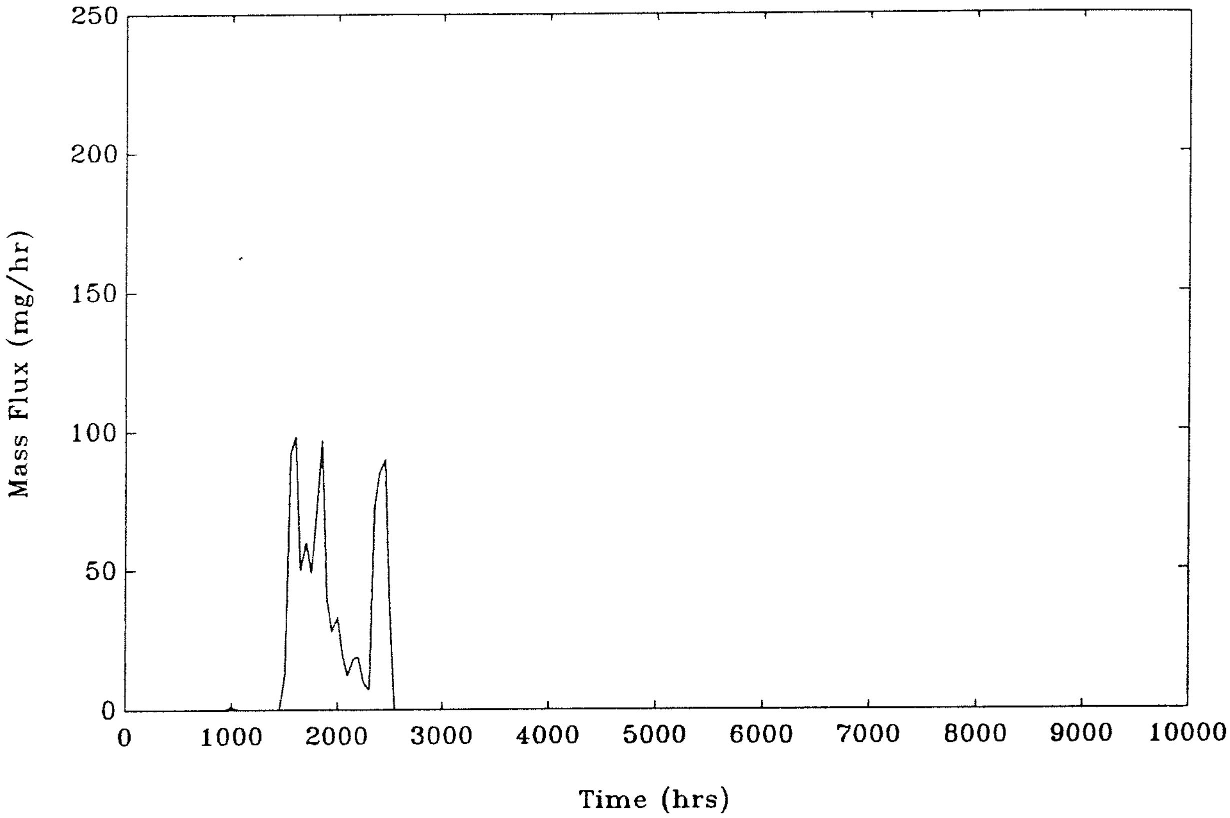

Figure 45 Field 96 breakthrough curve for far field simulation

List of SKB reports

Annual Reports

1977-78
TR 121
KBS Technical Reports 1 – 120
Summaries
Stockholm, May 1979

1979
TR 79-28
The KBS Annual Report 1979
KBS Technical Reports 79-01 – 79-27
Summaries
Stockholm, March 1980

1980
TR 80-26
The KBS Annual Report 1980
KBS Technical Reports 80-01 – 80-25
Summaries
Stockholm, March 1981

1981
TR 81-17
The KBS Annual Report 1981
KBS Technical Reports 81-01 – 81-16
Summaries
Stockholm, April 1982

1982
TR 82-28
The KBS Annual Report 1982
KBS Technical Reports 82-01 – 82-27
Summaries
Stockholm, July 1983

1983
TR 83-77
The KBS Annual Report 1983
KBS Technical Reports 83-01 – 83-76
Summaries
Stockholm, June 1984

1984
TR 85-01
Annual Research and Development Report 1984
Including Summaries of Technical Reports Issued during 1984. (Technical Reports 84-01 – 84-19)
Stockholm, June 1985

1985
TR 85-20
Annual Research and Development Report 1985
Including Summaries of Technical Reports Issued during 1985. (Technical Reports 85-01 – 85-19)
Stockholm, May 1986

1986
TR 86-31
SKB Annual Report 1986
Including Summaries of Technical Reports Issued during 1986
Stockholm, May 1987

1987
TR 87-33
SKB Annual Report 1987
Including Summaries of Technical Reports Issued during 1987
Stockholm, May 1988

1988
TR 88-32
SKB Annual Report 1988
Including Summaries of Technical Reports Issued during 1988
Stockholm, May 1989

1989
TR 89-40
SKB Annual Report 1989
Including Summaries of Technical Reports Issued during 1989
Stockholm, May 1990

1990
TR 90-46
SKB Annual Report 1990
Including Summaries of Technical Reports Issued during 1990
Stockholm, May 1991

1991
TR 91-64
SKB Annual Report 1991
Including Summaries of Technical Reports Issued during 1991
Stockholm, April 1992

Technical Reports
List of SKB Technical Reports 1992

TR 92-01
GEOTAB. Overview
Ebbe Eriksson[1], Bertil Johansson[2], Margareta Gerlach[3], Stefan Magnusson[2], Ann-Chatrin Nilsson[4], Stefan Sehlstedt[3], Tomas Stark[1]
[1]SGAB, [2]ERGODATA AB, [3]MRM Konsult AB
[4]KTH
January 1992

TR 92-02
Sternö study site. Scope of activities and main results
Kaj Ahlbom[1], Jan-Erik Andersson[2], Rune Nordqvist[2], Christer Ljunggren[3], Sven Tirén[2], Clifford Voss[4]
[1]Conterra AB, [2]Geosigma AB, [3]Renco AB,
[4]U.S. Geological Survey
January 1992

TR 92-03
Numerical groundwater flow calculations at the Finnsjön study site – extended regional area
Björn Lindbom, Anders Boghammar
Kemakta Consultants Co, Stockholm
March 1992

TR 92-04
Low temperature creep of copper intended for nuclear waste containers
P J Henderson, J-O Österberg, B Ivarsson
Swedish Institute for Metals Research, Stockholm
March 1992

TR 92-05
Boyancy flow in fractured rock with a salt gradient in the groundwater – An initital study
Johan Claesson
Department of Building Physics, Lund University, Sweden
February 1992

TR 92-06
Characterization of nearfield rock – A basis for comparison of repository concepts
Roland Pusch, Harald Hökmark
Clay Technology AB and Lund University of Technology
December 1991

TR 92-07
Discrete fracture modelling of the Finnsjön rock mass: Phase 2
J E Geier, C-L Axelsson, L Hässler, A Benabderrahmane
Golden Geosystem AB, Uppsala, Sweden
April 1992

TR 92-08
Statistical inference and comparison of stochastic models for the hydraulic conductivity at the Finnsjön site
Sven Norman
Starprog AB
April 1992

TR 92-09
Description of the transport mechanisms and pathways in the far field of a KBS-3 type repository
Mark Elert[1], Ivars Neretnieks[2], Nils Kjellbert[3], Anders Ström[3]
[1]Kemakta Konsult AB
[2]Royal Institute of Technology
[3]Swedish Nuclear Fuel and Waste Management Co
April 1992

TR 92-10
Description of groundwater chemical data in the SKB database GEOTAB prior to 1990
Sif Laurent[1], Stefan Magnusson[2], Ann-Chatrin Nilsson[3]
[1]IVL, Stockholm
[2]Ergodata AB, Göteborg
[3]Dept. of Inorg. Chemistry, KTH, Stockholm
April 1992

TR 92-11
Numerical groundwter flow calculations at the Finnsjön study site – the influence of the regional gradient
Björn Lindbom, Anders Boghammar
Kemakta Consultants Co., Stockholm, Sweden
April 1992

TR 92-12
HYDRASTAR – a code for stochastic simulation of groundwater flow
Sven Norman
Abraxas Konsult
May 1992

TR 92-13
Radionuclide solubilities to be used in SKB 91
Jordi Bruno[1], Patrik Sellin[2]
[1]MBT, Barcelona Spain
[2]SKB, Stockholm, Sweden
June 1992

TR 92-14
Numerical calculations on heterogeneity of groundwater flow
Sven Follin
Department of Land and Water Resources, Royal Institute of Technology
June 1992

TR 92-15
Kamlunge study site.
Scope of activities and main results
Kaj Ahlbom[1], Jan-Erik Andersson[2], Peter Andersson[2], Thomas Ittner[2], Christer Ljunggren[3], Sven Tirén[2]
[1]Conterra AB
[2]Geosigma AB
[3]Renco AB
May 1992

TR 92-16
Equipment for deployment of canisters with spent nuclear fuel and bentonite buffer in horisontal holes
Vesa Henttonen, Miko Suikki
JP-Engineering Oy, Raisio, Finland
June 1992

TR 92-17
The implication of fractal dimension in hydrogeology and rock mechanics
Version 1.1
W Dershowitz[1], K Redus[1], P Wallmann[1], P LaPointe[1], C-L Axelsson[2]
[1]Golder Associates Inc., Seattle, Washington, USA
[2]Golder Associates Geosystem AB, Uppsala, Sweden
February 1992

TR 92-18
Stochastic continuum simulation of mass arrival using a synthetic data set. The effect of hard and soft conditioning
Kung Chen Shan[1], Wen Xian Huan[1], Vladimir Cvetkovic[1], Anders Winberg[2]
[1] Royal Institute of Technology, Stockholm
[2] Conterra AB, Gothenburg
June 1992

TR 92-19
Partitioning and transmutation.
A review of the current state of the art
Mats Skålberg, Jan-Olov Liljenzin
Department of Nuclear Chemistry, Chalmers University of Technology
October 1992

TR 92-20
SKB 91
Final disposal of spent nuclear fuel. Importance of the bedrock for safety
SKB
May 1992

TR 92-21
The Protogine Zone.
Geology and mobility during the last 1.5 Ga
Per-Gunnar Andréasson, Agnes Rodhe
September 1992

TR 92-22
Klipperås study site.
Scope of activities and main results
Kaj Ahlbom[1], Jan-Erik Andersson[2], Peter Andersson[2], Tomas Ittner[2], Christer Ljunggren[3], Sven Tirén[2]
[1]Conterra AB
[2]Geosigma AB
[3]Renco AB
September 1992

TR 92-23
Bedrock stability in Southeastern Sweden. Evidence from fracturing in the Ordovician limestones of Northern Öland
Alan Geoffrey Milnes[1], David G Gee[2]
[1]Geological and Environmental Assessments (GEA), Zürich, Switzerland
[2]Geologiska Institutionen, Lund, Sweden
September 1992

TR 92-24
Plan 92
Costs for management of the radioactive waste from nuclear power production
Swedish Nuclear Fuel and Waste Management Co
June 1992

TR 92-25
Gabbro as a host rock for a nuclear waste repository
Kaj Ahlbom[1], Bengt Leijon[1], Magnus Liedholm[2], John Smellie[1]
[1]Conterra AB
[2]VBB VIAK
September 1992

TR 92-26
Copper canisters for nuclear high level waste disposal. Corrosion aspects
Lars Werme, Patrik Sellin, Nils Kjellbert
Swedish Nuclear Fuel and Waste Management Co, Stockholm, Sweden
October 1992

TR 92-27
Thermo-mechanical FE-analysis of butt-welding of a Cu-Fe canister for spent nuclear fuel
B L Josefson[1], L Karlsson[2], L-E Lindgren[2], M Jonsson[2]
[1]Chalmers University of Technology, Göteborg, Sweden
[2]Division of Computer Aided Design, Luleå University of Technology, Luleå, Sweden
October 1992

TR 92-28
A rock mechanics study of Fracture Zone 2 at the Finnsjön site
Bengt Leijon[1], Christer Ljunggren[2]
[1]Conterra AB
[2]Renco AB
January 1992

TR 92-29
Release calculations in a repository of the very long tunnel type
L Romero, L Moreno, I Neretnieks
Department of Chemical Engineering, Royal Institute of Technology, Stockholm, Sweden
November 1992

TR 92-30
Interaction between rock, bentonite buffer and canister. FEM calculations of some mechanical effects on the canister in different disposal concepts
Lennart Börgesson
Clay Technology AB, Lund Sweden
July 1992

TR 92-31
The Äspö Hard Rock Laboratory: Final evaluation of the hydro-geochemical pre-investigations in relation to existing geologic and hydraulic conditions
John Smellie[1], Marcus Laaksoharju[2]
[1]Conterra AB, Uppsala, Sweden
[2]GeoPoint AB, Stockholm, Sweden
November 1992

TR 92-32
Äspö Hard Rock Laboratory: Evaluation of the combined longterm pumping and tracer test (LPT2) in borehole KAS06
Ingvar Rhén[1] (ed.), Urban Svensson[2] (ed.), Jan-Erik Andersson[3], Peter Andersson[3], Carl-Olof Eriksson[3], Erik Gustafsson[3], Thomas Ittner[3], Rune Nordqvist[3]
[1]VBB VIAK AB
[2]Computer-aided Fluid Engineering
[3]Geosigma AB
November 1992

TR 92-33
Finnsjö Study site. Scope of activities and main results
Kaj Ahlbom[1], Jan-Erik Andersson[2], Peter Andersson[2], Thomas Ittner[2], Christer Ljunggren[3], Sven Tirén[2]
[1]Conterra AB
[2]Geosigma AB
[3]Renco AB
December 1992

TR 92-34
Sensitivity study of rock mass response to glaciation at Finnsjön, Central Sweden
Jan Israelsson[1], Lars Rosengren[1], Ove Stephansson[2]
[1]Itasca Geomekanik AB, Falun, Sweden
[2]Royal Institute of Technology, Dept. of Engineering Geology, Stockholm, Sweden
November 1992